



Australian Government  
Bureau of Meteorology

The Centre for Australian Weather and Climate Research  
A partnership between CSIRO and the Bureau of Meteorology

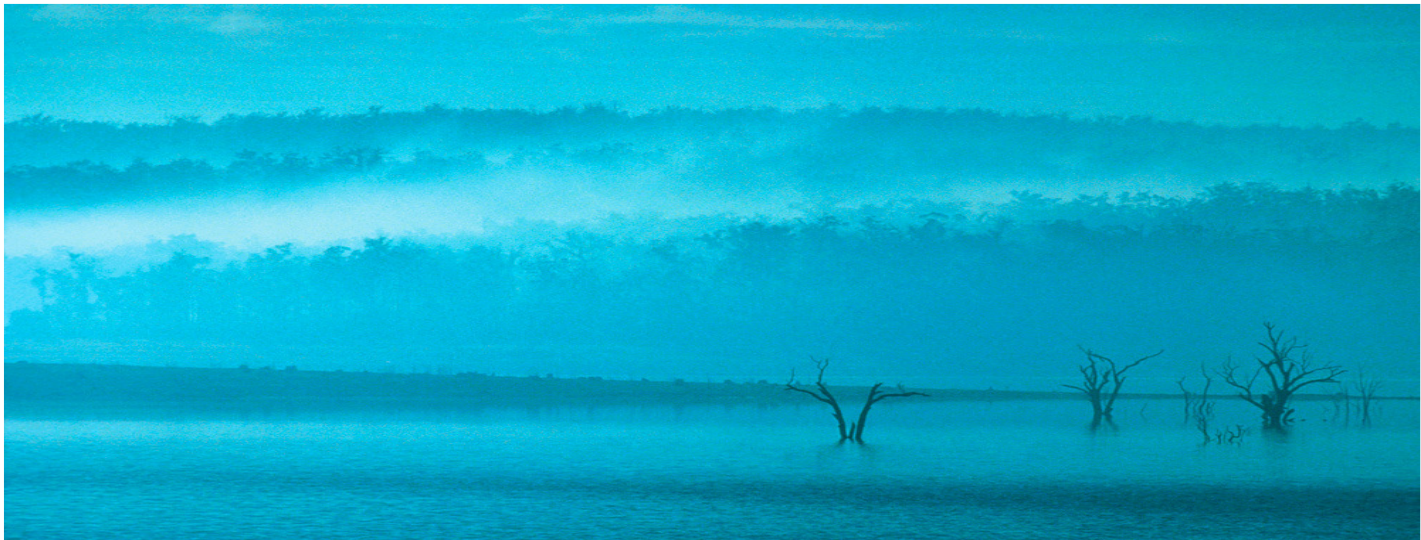


# The Bureau of Meteorology Statistical Downscaling Model Graphical User Interface: user manual and software documentation

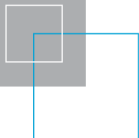
**CAWCR Technical Report No. 004**

B. Timbal, Z. Li and E. Fernandez

December 2008



[www.cawcr.gov.au](http://www.cawcr.gov.au)

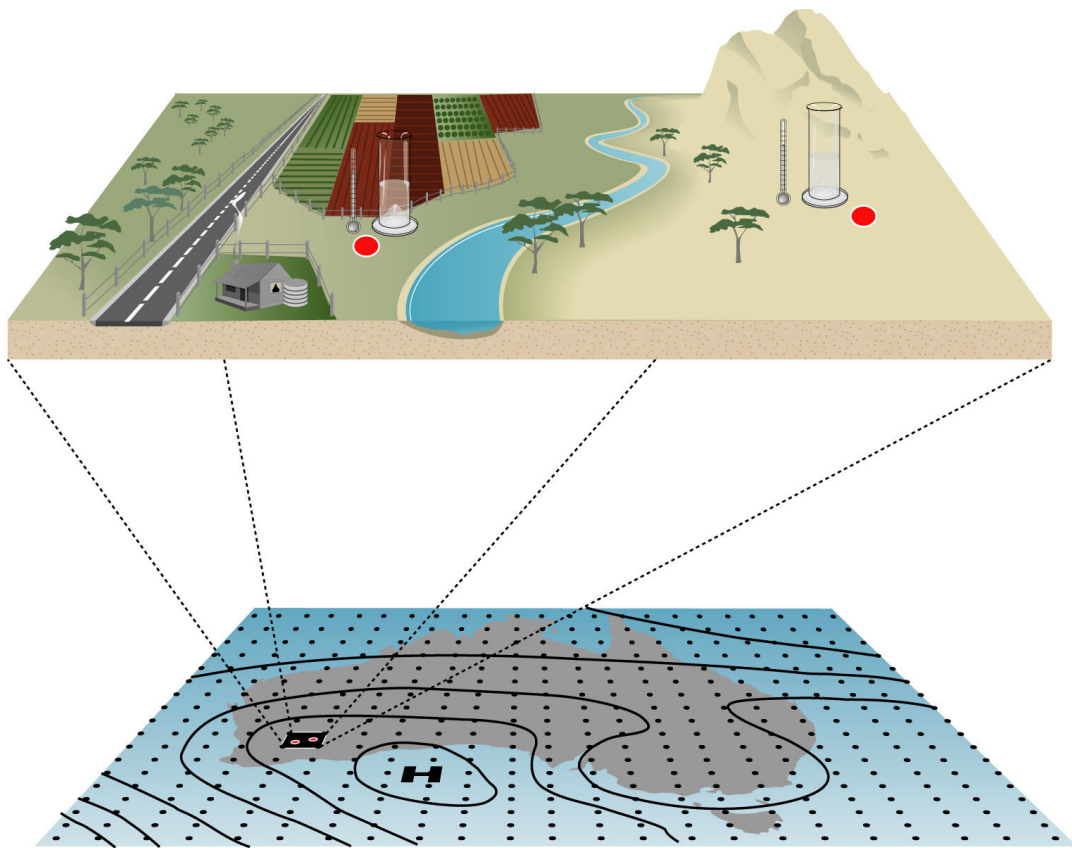




# The Bureau of Meteorology

## Statistical Downscaling Model

### Graphical User Interface



---

**User Manual  
&  
Software Documentation**

## Authorship

The Graphical User Interface (GUI) was developed in the research centre of the Bureau of Meteorology by **Zhihong Li**, under scientific guidance from **Bertrand Timbal**; during the course of the development, **Bradley Murphy** and **Elodie Fernandez** contributed to this work.

The documentation was compiled by B. Timbal, Z. Li and E. Fernandez.

The development of the Bureau of Meteorology statistical downscaling model (BoM-SDM) has long been supported by the **Department of Climate Change (DCC)** as part of the **Australian Climate Change Science Program (ACCSP)**.

While this CAWCR research report summarises the development of the BoM-SDM, as of the date of publication; the work is still on-going and users are encouraged to contact the authors to find out about the latest developments.

Enquiries should be addressed to:

Bertrand Timbal  
Centre for Australian Weather and Climate Research:  
A Partnership between the Bureau of Meteorology and CSIRO  
GPO Box 1289  
Melbourne VIC 3001  
AUSTRALIA  
[b.timbal@bom.gov.au](mailto:b.timbal@bom.gov.au)  
Phone: 61 3 9669 4697  
Fax: 61 3 9669 4660

ISSN: 1836-019X  
National Library of Australia Cataloguing-in-Publication

Timbal, Bertrand, 1970-

The Bureau of Meteorology statistical downscaling model graphical user interface [electronic resource] : user manual and software documentation / B. Timbal ; Z. Li ; E. Fernandez.

ISBN: 978-1-921424-77-9

Series: Technical report (Centre for Australian Weather and Climate Research.) ; no. 4.

Notes: Bibliography. Also issued in print.

1. Climatic changes—Mathematical models. 2. Statistical weather forecasting--Australia.

Other Authors/Contributors: Li, Zhihong; Fernandez, Elodie.

551.60994

## Copyright and Disclaimer

© 2008 CSIRO and the Bureau of Meteorology. To the extent permitted by law, all rights are reserved and no part of this publication covered by copyright may be reproduced or copied in any form or by any means except with the written permission of CSIRO and the Bureau of Meteorology.

CSIRO and the Bureau of Meteorology advise that the information contained in this publication comprises general statements based on scientific research. The reader is advised and needs to be aware that such information may be incomplete or unable to be used in any specific situation. No reliance or actions must therefore be made on that information without seeking prior expert professional, scientific and technical advice. To the extent permitted by law, CSIRO and the Bureau of Meteorology (including each of its employees and consultants) excludes all liability to any person for any consequences, including but not limited to all losses, damages, costs, expenses and any other compensation, arising directly or indirectly from using this publication (in part or in whole) and any information or material contained in it.

## Table of Contents

Abstract .....	1
Part A: Scientific background .....	3
1) Introduction .....	3
2) The Bureau of Meteorology Statistical Downscaling Model .....	4
3) The predictands obtained from the GUI .....	7
4) The development of the SDMs used in the GUI:.....	11
a) General principles guiding the optimisation of the SDMs.....	11
b) Defining daily meteorological situations .....	13
c) Change-of-Date files .....	15
d) SDM optimisation versus application to climate model simulations.....	15
e) Characteristics of the optimised SDMs: .....	17
5) Evaluation of the SDMs used in the GUI .....	20
6) The Global Climate Models used in the GUI .....	23
Part B: The Graphical User Interface.....	26
1) The software structure .....	26
f) Program flow chart .....	26
g) User management.....	27
h) Individual subroutines.....	28
2) Using the GUI.....	29
a) Access URL .....	29
b) Front page layout .....	29
c) The interactive web interface.....	30

3) Results provided by the GUI.....	34
a) Generating several outputs.....	34
b) Graphics and Data Display and Download.....	35
c) Termination and closing .....	37
4) Summary and additional information .....	39
a) Summary on the existing tool .....	39
b) Case studies performed with this tool.....	40
c) Future developments of the tool .....	40
d) Other existing software complementary to this tool.....	42
Acknowledgements.....	43
Bibliography .....	44
Appendix A: Analysis of the SDM optimised parameters.....	49
Appendix B: Analysis of the SDM skill .....	56
Appendix C: Perl scripts .....	66
Appendix D: Directory structure .....	70
Appendix E: The Statistical Downscaling Model (SDM) .....	73
Appendix F: The graphical outputs.....	79
Appendix G: Case study 1: projected Tmax in Mildura.....	83
Appendix H: Case study 2: sub-grid heterogeneity .....	87
a) For temperature .....	87
b) For rainfall .....	89

## Abstract

Climate change information required for impact studies is of a much finer spatial scale than climate models can directly provide. Statistical downscaling models (SDMs) are commonly used to fill this scale gap. SDMs are based on the view that the regional climate is conditioned by two factors: (1) the large scale climatic state and (2) local physiographic features. A SDM based on an analogue approach has been developed within the Australian Bureau of Meteorology and applied to ten regions covering the entire Australian continent. Six surface predictands (daily minimum and maximum temperatures, dew-point minimum and maximum temperatures, total rainfall and pan evaporation) were modelled. The skill of the SDMs was evaluated by comparing reconstructed and observed series using a range of metrics: the first two moments of the series, and the ability to reproduce day-to-day variability, inter-annual variability, and long-term trends. Once optimized, the SDMs were applied to a selection of global climate models which contributed to the Intergovernmental Panel on Climate Change 4<sup>th</sup> assessment report released in 2007. A user-friendly graphical interface has been developed to facilitate dissemination of the SDM results and provides a range of options for users to obtain tailored information. Once the projections are calculated for the places of interest, graphical outputs are displayed. These can be downloaded jointly with the underlying data, allowing users to manipulate the data in their own applications.

This document provides the user with both a description of the SDM and a user manual of the Graphical User Interface (GUI). The first part describes the scientific background: the objectives of downscaling and how the BoM SDM was developed, as well as the predictands obtained, how the model was optimised and evaluated and the global climate models used for projections. The second part is a comprehensive documentation of the GUI: its structure, usage and the results provided. The appendices provide more details about the optimised parameters of the model, its skill, the GUI Perl scripts and directory structure, the SDM structure and routines, and the graphical outputs of the GUI. The last appendix illustrates the benefits of the SDM via two case studies: projected maximum temperature in Mildura and sub-grid heterogeneity.



## Part A: Scientific background

### 1) Introduction

Global climate models (GCMs) have resolutions of hundreds of kilometres, whilst regional climate models (RCMs) may be as fine as tens of kilometres. However, impact assessment applications often require point-specific climate projections in order to capture fine-scale climate variations, particularly in regions with complex topography, coastal or island locations, and in areas of highly heterogeneous land-cover. Therefore a gap exists between what climate models can predict about future climate change and the information relevant for environmental studies. Statistical Downscaling Models (SDMs) are commonly used to fill this gap.

SDMs are based on the premise that the regional climate is conditioned by two factors: the large-scale climatic state and local physiographic features. From this perspective, regional or local climate information is derived by first determining a statistical model which relates large-scale climate variables (or “predictors”) to regional and local variables (or “predictands”). Once this relationship is established, the large-scale output of GCM simulations can be fed into the statistical model to estimate the corresponding local and regional climate characteristics. There have been numerous applications of SDMs, both in Australia and elsewhere. According to the latest IPCC assessment: “*Research on SDM has shown an extensive growth in application, and includes an increased availability of generic tools for the impact community*” (pp 920, Chapter 11, IPCC 4<sup>th</sup> assessment, Christensen et al., 2007). In light of this ongoing trend, the Bureau of Meteorology Statistical Downscaling Model has been extended to cover most of the Australian continent, and in order to facilitate access to downscaling projections across a broader user community, a graphical user interface (GUI) that provides projections across the southern half of the Australian continent has been developed. The GUI is a web-based tool using a combination of static HTML (HyperText Markup Language) pages and dynamically-generated pages. It provides users with access to projections for a series of surface predictands at point-specific locations.

## 2) The Bureau of Meteorology Statistical Downscaling Model

The Australian Bureau of Meteorology (BoM) has developed a SDM using the idea of a meteorological analogue (Timbal and McAvaney, 2001). This is one example of a more general type of SDM based on weather classification methods in which predictands are chosen by matching previous (i.e., analogous) situations to the current weather-state. The method was originally designed for weather forecasting applications (Lorenz, 1969) but was abandoned due to its limited success and lack of suitable analogues for systems with large degrees of freedom (Van Den Dool, 1994). The popularity of the method has recently increased with the availability of datasets covering longer time periods following the completion of several reanalysis projects and the recognition that the dimension of the search space (i.e. the spatial domain and the number of predictors) must be suitably restricted when identifying analogues. The analogue method still performs poorly when the pool of training observations is limited and/or the number of classifying predictors is large.

The BoM SDM was first developed for daily maximum and minimum temperatures ( $T_{\max}$  and  $T_{\min}$ ) across the Murray-Darling Basin (MDB) in Australia (Timbal and McAvaney, 2001). The choice of a single, best analogue is based on a closest neighbour using a simple Euclidean metric. The metric is applied to a single vector which comprises daily normalised anomalies of point values within an optimised geographical area for the selected predictors. The choice of the optimal combination of predictors and the geographical area are two key steps in the optimisation of the analogue model. The SDM was then extended to rainfall occurrences (Timbal *et al.*, 2003) and amount (Timbal, 2004). During these applications, the technique was tested on other mid-latitude geographical areas in both Australia and Europe.

The ability of the SDM to reproduce shifts in the observed climate, a proxy for its ability to reproduce the shift in current climate due to global warming, has been tested for the rainfall decline in the late 1960s in the Southwest of Western Australia (SWA, Timbal, 2004) and in the mid 1990s in the Southwest of Eastern Australia (SEA, Timbal and Jones, 2008). It shows that the method is able to capture observed rainfall

step changes providing that the appropriate large-scale forcings are used. In both cases, besides the synoptic, dynamic and thermal variables, the optimal combination of predictors must include a moisture related variables. Furthermore, downscaled projections from the BoM-SDM were compared with direct model outputs and were shown to be consistent when averaged back on a scale relevant to climate model resolution (Timbal *et al.*, 2008b).

The technique was also used to enhance the signal in the classic signal-to-noise problem, that is, the possible attribution to external causes of an observed change detected as significant. In the case of the rainfall decline in SWA, using the SDM it was possible to partly attribute this decline to greenhouse gases and other large-scale emissions (Timbal *et al.*, 2006), with an additional contribution from regional land clearance (Timbal and Arblaster, 2006).

Although the ability of the statistical linkage to reproduce non-stationary climates has been thoroughly tested in several instances, it is one of several limitations often cited as possible short-comings of SDMs (Hewitson and Crane, 2006; Christensen *et al.*, 2007). Users should be familiar with these issues and possible limitations in using downscaled outputs as discussed as discussed in Timbal (2006a):

- That large-scale predictors, relevant to the local predictands are adequately reproduced by the climate models;
- That the statistical relationship between predictors and predictands is stable and valid in a warmer world; and
- That the chosen predictors encompass all the climate change signals.

Users should also be aware of the important benefit provided by SDMs compared to using Direct Model Outputs (DMOs); more complete discussions on the advantages can be found in Timbal (2006b):

- Provide local climate change information;
- By-pass some of the physical parameterizations used to calculate model predictands, which are also subject to fitting to observed data (as do SDMs);
- Provide a cost-effective way to describe the cascade of uncertainties relevant to local climate change projections.

And finally, it is recommended that users of downscaled projections are informed about the *best practices* in this area. E.g. the IPCC (Wilby et al., 2004) has established a guideline which is very relevant to users of the GUI described here.

### 3) The predictands obtained from the GUI

For surface predictands, the best possible stations available for long-term climate purposes are the High Quality (HQ) dataset assembled by the National Climate Centre (NCC) from the Bureau of Meteorology. Variables used were daily HQ temperature extremes (Trewin, 2001) and daily HQ rainfall amount (Lavery *et al.*, 1992 and 1997). Both datasets were extended to 2005 by the NCC. More recently HQ datasets were developed for surface humidity (dew point daily extremes  $dT_{\min}$  and  $dT_{\max}$ ) by Lucas (2006) and for surface pan evaporation (pE) (Jovanovic *et al.*, 2008). Following on the early work on temperature and rainfall, the SDM was optimised for the new HQ network (Timbal *et al.*, 2008). Therefore downscaled projections for 6 surface predictands can currently be obtained through the GUI:

- ✓ **Rainfall**
- ✓  **$T_{\max}$**
- ✓  **$T_{\min}$**
- ✓ **pE**
- ✓  **$dT_{\max}$**
- ✓  **$dT_{\min}$**

The technique was first extended to the entire extra-tropical half of the Australian continent, generally south of 33°S (Timbal *et al.*, 2008a) and more recently to the Tropical half of the Australian continent. It has then been applied to the latest round of GCM projections for the 21<sup>st</sup> century, which were assembled as part of the 4<sup>th</sup> Assessment of the Intergovernmental Panel on Climate Change (IPCC). The continent was separated into ten distinct climate entities (Fig. 1), roughly following the rotated Empirical Orthogonal Functions (EOFs) for rainfall suggested by Drosowsky (1993):

1. The Southwest of Western Australia (**SWA**): similar to the Indian Ocean Climate Initiative (IOCI) triangle (IOCI, 1999), south of a north boundary from Geraldton to Kalgoorlie (about 30°S) and west of a line from Kalgoorlie to Esperance (about 122°E);

- The Nullarbor (**NUL**) region: a vast region from the SWA in the west and the Eyre Peninsula in South Australia in the east (about 136°E), and from the coast to 30°S. This area has very few high quality observations and therefore its optimisations are likely to be the least successful;

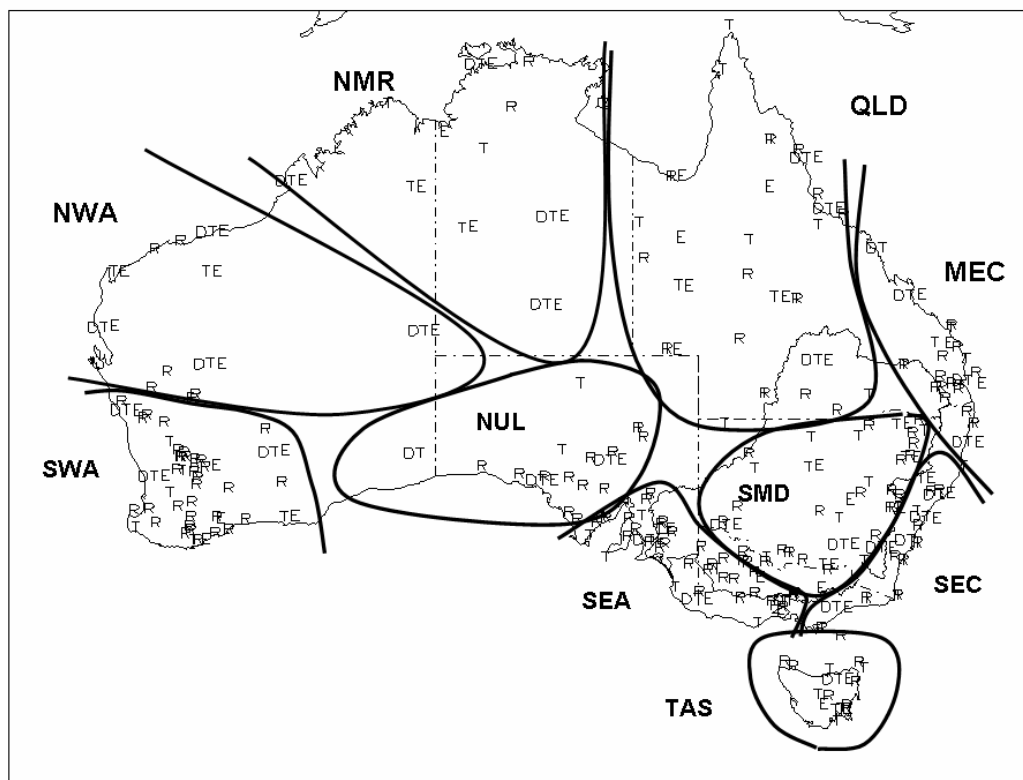


**Fig 1:** Location of the high quality networks across Australia for rainfall (R), temperature (T), dew-point temperature (D) and pan evaporation (E). The boundaries of the ten areas of interest are overlaid: Tasmania (TAS), Southwest of Western Australia (SWA), Nullarbor Plain (NUL), the Southwest of Eastern Australia (SEA), the Southern part of the Murray-Darling basin (SMD), the South-East Coast (SEC), the Mid-East Coast (MEC), Queensland (QLD), the Northern Monsoon Region (NMR) and the Northwest of Western Australia (NWA) .

- The Southwest of Eastern Australia (**SEA**): southwest of a line from Melbourne (38°S and 145°E) to Port Augusta (33°S and 138°E), this area was identified as the centre of the early winter rainfall decline and having strong similarities with the SWA (Timbal and Jones, 2008);
- The Southern half of the Murray-Darling Basin (**SMD**) limited to about 33°S in the north, limited in the west by the line described earlier separating the region from the SEA, and limited in the east by the Great Dividing Range (GDR);

5. The South-East Coast (**SEC**): the coastal band east of the GDR from Wilson Promontory in Victoria in the south, all the way along the NSW coast up to the Queensland border;
6. The island of Tasmania (**TAS**), including all Bass Strait islands;
7. The Northwest of Western Australia (**NWA**): limited in the south by the line described earlier as the northern boundary of SWA region, in the north by a line from Port Headland to Yulara (in NT) and in the west by the WA state border (about 129 °E); and
8. The Northern monsoon region (**NMR**): limited in the south by the northern boundary of NWA region and by the NT state border (about 26 °S) and in the west by the 136 °E meridian;
9. The Mid-East Coast (**MEC**): the coastal band east of a line from Mackay in QLD to Port Macquarie in NSW; and
10. The Queensland state (**QLD**), excluding its southeast corner which is included in the MEC region.

The number of surface predictands available for each climatic region is summarised in Table 1.

Predictands	TAS	SWA	NUL	SEA	SMD	SEC	MEC	NWA	NMR	QLD
Temperature	7	9	5	11	15	13	11	6	7	17
Rainfall	8	34	12	31	24	9	12	5	2	12
Pan evap.	3	7	2	5	9	7	5	4	7	9
Dew point	1	3	3	3	2	7	4	4	4	3

**Table 1:** *Number of stations for every predictand and in each climatic region; and the sum of these stations in the ten regions represented as a percentage of the corresponding entire high quality network (last column).*

#### **4) The development of the SDMs used in the GUI:**

##### **a) General principles guiding the optimisation of the SDMs**

The development and validation of the SDM was performed using the highest quality data available for both surface predictands and large-scale predictors, as it is important to ensure that data quality does not impact the statistical linkage being developed.

Global re-analyses of the atmosphere were used for the large-scale predictors. Both the NCEP/NCAR re-analysis datasets (NNR), available from 1948 to present (Kalnay *et al.*, 1996), and the European Centre (ECMWF) ERA40 re-analysis datasets, available from 1957 to 2003 (Uppala *et al.*, 2005), were used to test the SDM. The impact of data quality on the SDM performance was carefully assessed. It was found that NNR from 1958 to 2005 (i.e. withdrawing the earlier decade from 1948 to 1957) provided the best results. Overall the SDM skill was higher when the NNR were used rather than ERA40, suggesting that NNR is more reliable above the Australian continent over the length of the record. Therefore, NNR from 1958 to 2005 are used as the reference database to search for analogues of the global climate models used in the GUI.

A total of 192 SDMs were produced: six predictands in six regions and three predictands in the four tropical regions, one for each four calendar season – summer (DJF), autumn (MAM), winter (JJA) and spring (SON). Each individual SDM was optimised using a range of statistics. These covered the ability of the SDM to reproduce mean and variance of the observed Probability Density Function (PDF) of the series, and the skill of the model in reproducing day-to-day variability, inter-annual variability (both using correlations) and long-term linear trends.

In each of the 192 cases, determining the best statistical scheme to use (i.e. the optimisation of the SDM) was based on a subjective analysis of the various metrics listed above. No attempt was made to develop an objective approach to obtain the optimal combination of predictors. Several reasons can be listed to justify allowing for expert assessment:

- Predictors are not strictly independent and therefore, their importance as a single predictor is not necessarily a good guide for their contribution in a combination of predictors due to their inter-dependence;
- It is generally not the case that a single combination of predictors will yield superior results for all metrics used and hence a trade-off exists between the importance of the various predictors and their role;
- The choice of predictors is also driven by the reliability of these variables in climate models.

For all these reasons, it was decided that a subjective analysis of the optimal combination of predictors is the most effective way to optimise individual SDMs.

Each SDM was developed in two stages. In the first stage, the best combination of predictors was determined; in the second stage additional parameters were optimized. The BoM SDM includes a large number of choices and each could be considered as a tuneable parameter. However previous studies have shown that only three parameters are important in affecting the choice of analogues (Timbal, 2004) and were therefore systematically explored as part of the extension of the technique across the Australian continent:

1. The size of the geographical domain used for the predictors (latitude and longitude). Only two domain sizes, chosen a-priori based on previous studies, were tested.
2. The calendar window from which analogues are found. Three periods were tested; 15, 30 and 60 days prior to and after the model date.
3. The way the daily anomalies are calculated: using either three monthly values or a single seasonal average.

## b) Defining daily meteorological situations

Daily meteorological situations are summarised by a single vector (step 1 in Fig. 2) containing a value for every latitude-longitude point within the geographical domain chosen and for all the predictors selected (i.e. the vector length is equal to the size of the geographical domain -number of latitudes times number of longitudes- multiplied by the number of predictors). The mathematical need for a vector is to be able to combine different maps: one per predictor chosen as part of the optimised combination of predictors.

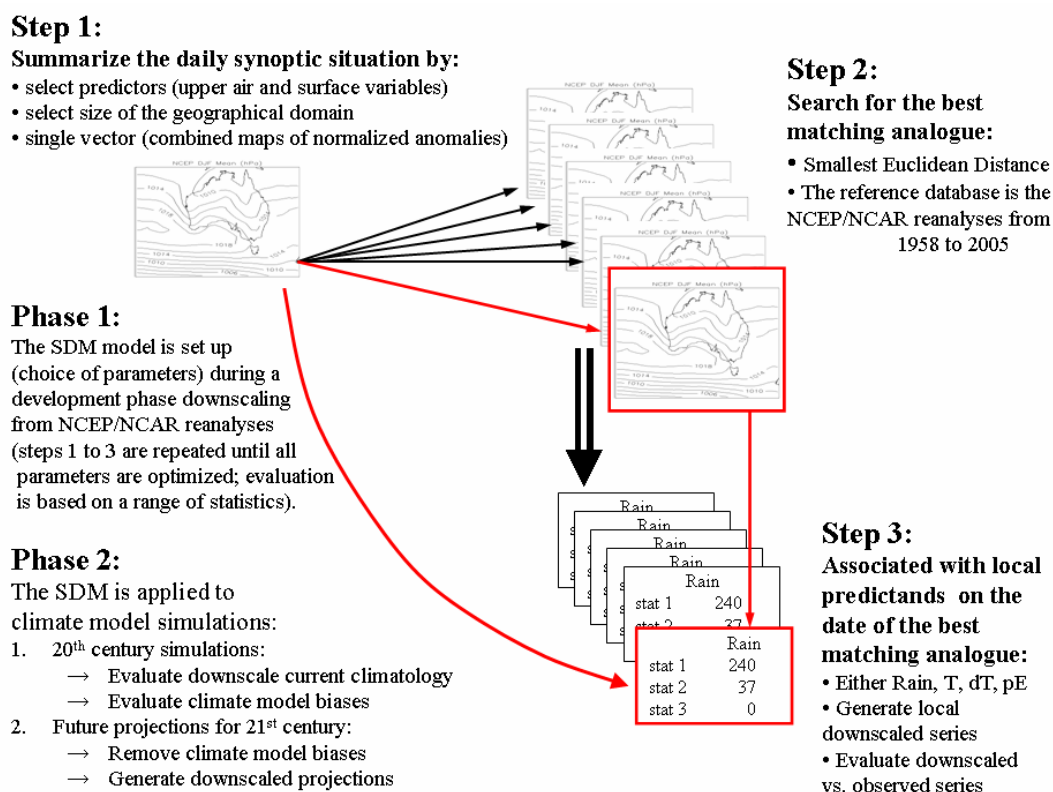


**Figure 2:** Schematic diagram of the methodology used to optimise (phase 1) and apply (phase 2) the Statistical Downscaling Model. The various steps involved to obtain meteorological analogues (steps 1 to 3) are described in the text.

Some manipulations of the elements of the vector are needed to ensure that all elements are “comparable” and hence have equal weight when it comes to finding the best matching analogue. Every element of the vector formed is a daily normalised anomaly calculated from the long-term climatology (either using monthly or seasonal means). All elements of the vector are therefore dimensionless, with a mean of zero and a standard deviation of 1 (over the length of the period of interest for which analogues are searched for).

Each vector formed (one per daily meteorological situation of the period of interest) is then compared to similar vectors formed for every daily meteorological situation in the reference database: the reference database is the NNR from 1958 to 2005.

The search for the optimal analogue is conducted using Euclidean distance between vectors. The smallest Euclidean distance (i.e. the sum of the squares of the differences between each element of the two vectors being compared) defines the best matching analogue providing it is within the requirements in terms of calendar window (step 2 in Fig. 2). A “best matching analogue” is calculated for every single day of the period of interest and kept in change-of-date (COD) files. The period of interest is also 1958 to 2005 for the development phase but differs when the SDM is applied to climate simulations (i.e. different time-slices during the 20<sup>th</sup> and 21<sup>st</sup> century).

It is worth noting that here the optimisation of the SDM (i.e. the repetition of steps 1 to 3 until the statistics used show the highest skill for the SDM) was not done in a full cross-validated manner to ensure that the largest dataset could be used. The reference database and period of interest are both the entire 1958 to 2005 period, but analogues are not allowed to come from the same calendar year (or consecutive December, January and February in the case of summer). This provision is to ensure that no artificial skill is introduced in the SDM (i.e. due to seasonal anomalies not captured by atmospheric large-scale forcings such as soil moisture). This decision was based on previous developments of the SDM using fully cross-validated methodology (Timbal and McAvaney, 2001; Timbal *et al.*, 2003; Timbal, 2004).

### **c) Change-of-Date files**

Whenever the SDM is run, the main output is the COD file where the optimal analogue for every meteorological situation for the period of interest is kept. COD files contain as many lines as there are days in the period of interest, and three columns: the first one contains the date for which analogues were search for, the second column contains the date of the best matching analogue and the third column contains the Euclidean distance (providing a measure of the closeness of the best matching analogue). From this COD file, local predictands are calculated by using the observed values in the desired location for the date given as the best matching analogue (step 3 in Fig. 2).

A consequence of this methodology is that once the SDM has been optimised for a particular season/region/variable using HQ networks (to ensure that data quality does not affect the choice of parameters optimisation of the SDM), the COD file becomes independent of the predictand database. Therefore it is applicable to any other observations provided they are within the same region and of the same meteorological variable. That feature makes possible extensions of the tool to user-chosen datasets as well as gridded observations (future perspectives for the BoM-GUI are discussed in the *Summary and additional information* section). More details on the COD files and how they are used by the GUI are provided in Appendix E.

### **d) SDM optimisation versus application to climate model simulations**

The same method (minimisation of the Euclidean distance to find the best matching analogue) is used during the optimisation of the SDM (Phase 1 in Fig. 2) and for its application to climate model simulations (Phase 2 in Fig. 2). Both phase 1 and 2 include all three steps; but once the SDM has been optimised for a particular season/region/variable, the choice of parameters (predictors, and additional parameters) is “frozen” when applied to model simulations.

The SDM is always applied first to simulations of time-slices of the current climate (i.e. the latter part of the 20<sup>th</sup> century) so that the reliability of the downscaling for a particular climate model can be assessed. Although the SDM removes some of the biases affecting climate models, the objective of a statistical downscaling method is not to correct a poorly performing climate model but to “translate” large-scale circulation simulated by the climate model to the local scale relevant for an impacts study. Therefore, the ability of the climate model to represent realistically the large-scale circulation is relied upon, and any inaccuracies in the climate model will affect the downscaled predictand series and the appropriateness of the local series for impact studies has to be evaluated.

This step is also required to deal with the mean biases from climate model simulations. During the application of the SDM to simulations of the current climate, model biases (mean climatology and daily variability) are removed when predictors are normalised. The mean climatology of the control simulation which includes the climate model “drift” is kept as well as the standard deviation.

When the SDM is applied to simulations of future climate, the normalisation of the predictors is made using means and standard deviations calculated from the simulations of the 20<sup>th</sup> century rather than the future scenarios. This two stages approach is needed to factor into the daily anomalies the climate change signal (i.e. the difference between the climatology of the simulation of the 20<sup>th</sup> century versus the future projections) and to remove the model drift (i.e.: the mean value for the 20<sup>th</sup> century simulation). This means that when the SDM is applied to future projections, the elements of the vector are not normal anymore (mean is not equal to zero and variance is not equal to one). That “abnormality” is due to the climate change signal affecting the predictors and is the source of the climate change signal that the SDM will generate for the downscaled projections.

**e) Characteristics of the optimised SDMs:**

A complete analysis of the results from the two optimization steps is provided in Appendix A; here we only present a summary of the best combination of predictors. The predictors considered were chosen based on experience acquired while developing the BoM SDM (Timbal and McAvaney, 2001; Timbal *et al.*, 2003; Timbal, 2004), evidence in the literature from other studies in similar areas (Charles *et al.*, 1999; 2003), and the availability of variables in the climate model database.

In most cases, the predictors are low-level atmospheric fields, but in some instances large-scale rainfall or  $T_{\max}$  or  $T_{\min}$  from the GCMs are used as predictors. The optimum combination of predictors varies across regions, seasons and predictands (Tables 2a for  $T_{\max}$ ,  $T_{\min}$  and rainfall and 2b for  $dT_{\max}$ ,  $dT_{\min}$  and pE)).

The predictors are defined as follows:

- ✓ MSLP is the Mean Sea Level Pressure (in hPa);
- ✓  $T_{\min}$  and  $T_{\max}$  are the surface min and max temperature (in °C);
- ✓ PRCP is the total rainfall (in mm);
- ✓ Q is the specific humidity (in g/Kg);
- ✓ R is the relative humidity (in %);
- ✓ T is the temperature(in °C);
- ✓ U and V are the zonal and meridional wind components (in m.s<sup>-1</sup>); and
- ✓ Subscript numbers indicate the atmospheric level for the variable in hPa.

		<b>T<sub>max</sub></b>	<b>T<sub>min</sub></b>	<b>Rain</b>
<b>SWA</b>	Summer	MSLP & T <sub>850</sub> & V <sub>850</sub>	MSLP & T <sub>850</sub> & Q <sub>850</sub> & U <sub>850</sub>	MSLP & PRCP & Q <sub>850</sub> & U <sub>850</sub>
	Autumn	MSLP & T <sub>850</sub> & V <sub>850</sub>	MSLP & T <sub>850</sub> & Q <sub>850</sub> & U <sub>850</sub>	MSLP & PRCP & Q <sub>850</sub> & U <sub>850</sub>
	Winter	MSLP & T <sub>850</sub> & V <sub>850</sub>	MSLP & T <sub>850</sub> & Q <sub>850</sub>	MSLP & Q <sub>850</sub> & U <sub>850</sub>
	Spring	MSLP & T <sub>850</sub> & V <sub>850</sub>	MSLP & T <sub>850</sub> & Q <sub>850</sub>	MSLP & Q <sub>850</sub> & U <sub>850</sub>
<b>NUL</b>	Summer	MSLP & T <sub>850</sub> & V <sub>850</sub>	MSLP & T <sub>850</sub> & Q <sub>850</sub>	MSLP & PRCP & Q <sub>850</sub> & U <sub>850</sub>
	Autumn	MSLP & T <sub>850</sub> & V <sub>850</sub>	T <sub>850</sub> & Q <sub>850</sub>	MSLP & T <sub>850</sub> & Q <sub>850</sub> & U <sub>850</sub>
	Winter	MSLP & T <sub>850</sub> & U <sub>850</sub>	MSLP & T <sub>850</sub> & Q <sub>850</sub> & U <sub>850</sub>	MSLP & T <sub>850</sub> & Q <sub>850</sub> & U <sub>850</sub>
	Spring	MSLP & T <sub>850</sub> & V <sub>850</sub>	T <sub>850</sub> & Q <sub>850</sub>	MSLP & Q <sub>850</sub> & T <sub>850</sub>
<b>SEA</b>	Summer	MSLP & T <sub>850</sub>	MSLP & T <sub>850</sub>	MSLP & PRCP & T <sub>850</sub>
	Autumn	MSLP & T <sub>max</sub>	MSLP & T <sub>850</sub> & Q <sub>850</sub>	MSLP & T <sub>max</sub> & Q <sub>850</sub> & U <sub>850</sub>
	Winter	MSLP & T <sub>850</sub> & T <sub>max</sub> & U <sub>850</sub>	MSLP & T <sub>850</sub> & Q <sub>850</sub>	MSLP & PRCP & V <sub>850</sub>
	Spring	U <sub>850</sub>	MSLP & T <sub>850</sub> & Q <sub>850</sub>	MSLP & PRCP
<b>SMD</b>	Summer	MSLP & T <sub>max</sub>	T <sub>850</sub> & Q <sub>850</sub>	MSLP & PRCP & V <sub>850</sub>
	Autumn	MSLP & T <sub>max</sub>	T <sub>850</sub> & Q <sub>850</sub>	MSLP & PRCP & V <sub>850</sub>
	Winter	MSLP & T <sub>850</sub> & T <sub>max</sub> & U <sub>850</sub>	MSLP & T <sub>850</sub> & Q <sub>850</sub>	MSLP & PRCP & V <sub>850</sub>
	Spring	U <sub>850</sub>	MSLP & T <sub>850</sub> & Q <sub>850</sub>	MSLP & PRCP & V <sub>850</sub>
<b>SEC</b>	Summer	MSLP & T <sub>max</sub>	MSLP & T <sub>850</sub> & Q <sub>850</sub>	MSLP & T <sub>max</sub> & Q <sub>850</sub> & U <sub>850</sub>
	Autumn	MSLP & T <sub>max</sub>	MSLP & T <sub>850</sub> & Q <sub>850</sub>	MSLP & PRCP & Q <sub>850</sub> & U <sub>850</sub>
	Winter	MSLP & T <sub>max</sub>	MSLP & T <sub>850</sub> & T <sub>min</sub> & U <sub>850</sub>	MSLP & PRCP & U <sub>850</sub>
	Spring	MSLP & T <sub>850</sub> & T <sub>max</sub> & U <sub>850</sub>	MSLP & T <sub>850</sub> & Q <sub>850</sub>	MSLP & PRCP & Q <sub>850</sub> & U <sub>850</sub>
<b>TAS</b>	Summer	MSLP & T <sub>850</sub> & T <sub>max</sub> & U <sub>850</sub>	MSLP & T <sub>850</sub> & Q <sub>850</sub>	MSLP & Q <sub>850</sub> & V <sub>850</sub>
	Autumn	MSLP & T <sub>850</sub> & T <sub>max</sub> & U <sub>850</sub>	MSLP & T <sub>850</sub> & Q <sub>850</sub>	MSLP & Q <sub>850</sub> & V <sub>850</sub>
	Winter	MSLP & T <sub>850</sub> & Q <sub>850</sub> & U <sub>850</sub>	MSLP & T <sub>850</sub> & T <sub>min</sub> & U <sub>850</sub>	MSLP & PRCP & Q <sub>850</sub> & U <sub>850</sub>
	Spring	MSLP & T <sub>850</sub> & T <sub>max</sub> & U <sub>850</sub>	MSLP & T <sub>850</sub> & T <sub>min</sub> & U <sub>850</sub>	MSLP & PRCP & Q <sub>850</sub> & U <sub>850</sub>
<b>NWA</b>	Summer	T <sub>850</sub> & U <sub>850</sub> & T <sub>max</sub>	T <sub>850</sub> & Q <sub>850</sub>	PRCP & V <sub>700</sub> & R <sub>850</sub>
	Autumn	T <sub>850</sub> & V <sub>700</sub> & T <sub>max</sub>	T <sub>850</sub> & Q <sub>700</sub>	PRCP
	Winter	T <sub>850</sub> & T <sub>max</sub>	T <sub>850</sub> & T <sub>min</sub> & Q <sub>850</sub>	PRCP & Q <sub>850</sub>
	Spring	T <sub>850</sub>	T <sub>850</sub> & Q <sub>700</sub> & T <sub>min</sub>	PRCP & R <sub>700</sub>
<b>QLD</b>	Summer	T <sub>850</sub> & U <sub>850</sub> & T <sub>max</sub>	T <sub>min</sub>	PRCP
	Autumn	T <sub>max</sub>	T <sub>min</sub>	PRCP & T <sub>max</sub> & V <sub>850</sub>
	Winter	T <sub>max</sub> & MSLP	T <sub>min</sub>	PRCP
	Spring	T <sub>850</sub> & Q <sub>850</sub> & T <sub>max</sub>	T <sub>850</sub> & Q <sub>850</sub> & T <sub>min</sub>	PRCP
<b>NMR</b>	Summer	T <sub>850</sub> & T <sub>max</sub>	T <sub>850</sub> & Q <sub>850</sub>	PRCP
	Autumn	T <sub>850</sub> & T <sub>max</sub>	T <sub>850</sub> & T <sub>min</sub> & Q <sub>850</sub>	PRCP & U <sub>850</sub> & T <sub>max</sub>
	Winter	T <sub>850</sub> & Q <sub>850</sub> & U <sub>850</sub>	T <sub>850</sub> & Q <sub>850</sub>	PRCP
	Spring	T <sub>850</sub>	T <sub>850</sub> & Q <sub>850</sub> & T <sub>min</sub>	PRCP
<b>MEC</b>	Summer	T <sub>850</sub> & U <sub>850</sub> & T <sub>max</sub>	T <sub>min</sub>	MSLP & T <sub>max</sub> & R <sub>700</sub>
	Autumn	T <sub>850</sub> & U <sub>850</sub> & T <sub>max</sub>	T <sub>min</sub>	PRCP & Q <sub>850</sub> & U <sub>850</sub> & V <sub>850</sub>
	Winter	MSLP & T <sub>max</sub>	T <sub>min</sub>	MSLP & R <sub>850</sub> & V <sub>850</sub>
	Spring	T <sub>850</sub> & R <sub>850</sub>	T <sub>850</sub> & Q <sub>850</sub>	R <sub>850</sub> & T <sub>max</sub> & U <sub>850</sub>

**Table 2a:** Optimum combination of parameters for each calendar season and the ten regions for T<sub>min</sub>, T<sub>max</sub> and Rainfall.

		<b>pE</b>	<b>dT<sub>max</sub></b>	<b>dT<sub>min</sub></b>
<b>SWA</b>	Summer	MSLP & T <sub>max</sub> & R <sub>925</sub>	Q <sub>850</sub> & T <sub>min</sub>	Q <sub>925</sub> & T <sub>min</sub>
	Autumn	MSLP & T <sub>850</sub> & R <sub>850</sub>	MSLP & Q <sub>925</sub> & T <sub>min</sub>	Q <sub>925</sub> & T <sub>min</sub>
	Winter	MSLP & T <sub>max</sub> & R <sub>925</sub>	MSLP & Q <sub>850</sub> & T <sub>min</sub>	Q <sub>925</sub> & T <sub>min</sub>
	Spring	MSLP & T <sub>max</sub> & R <sub>850</sub>	Q <sub>850</sub> & T <sub>850</sub>	Q <sub>925</sub> & T <sub>min</sub>
<b>NUL</b>	Summer	T <sub>850</sub> & R <sub>925</sub>	MSLP & Q <sub>925</sub> & T <sub>min</sub>	MSLP & Q <sub>925</sub> & T <sub>min</sub>
	Autumn	T <sub>850</sub> & R <sub>925</sub>	MSLP & Q <sub>925</sub>	MSLP & Q <sub>925</sub>
	Winter	T <sub>max</sub> & R <sub>925</sub>	MSLP & Q <sub>925</sub> & T <sub>min</sub>	MSLP & Q <sub>925</sub> & T <sub>850</sub>
	Spring	T <sub>850</sub> & R <sub>925</sub>	MSLP & Q <sub>925</sub> & T <sub>min</sub>	Q <sub>925</sub>
<b>SEA</b>	Summer	T <sub>max</sub> & R <sub>925</sub>	MSLP & Q <sub>925</sub>	MSLP & Q <sub>925</sub> & T <sub>min</sub>
	Autumn	T <sub>max</sub> & R <sub>925</sub>	MSLP & Q <sub>925</sub> & T <sub>min</sub> & V <sub>850</sub>	MSLP & Q <sub>925</sub> & T <sub>min</sub>
	Winter	T <sub>max</sub> & R <sub>925</sub>	MSLP & Q <sub>925</sub> & T <sub>min</sub>	MSLP & Q <sub>925</sub> & T <sub>min</sub>
	Spring	T <sub>max</sub> & R <sub>925</sub>	MSLP & Q <sub>925</sub> & T <sub>min</sub>	MSLP & Q <sub>925</sub> & T <sub>min</sub>
<b>SMD</b>	Summer	T <sub>max</sub> & R <sub>850</sub>	MSLP & Q <sub>850</sub> & T <sub>min</sub> & V <sub>850</sub>	MSLP & Q <sub>850</sub> & T <sub>850</sub>
	Autumn	T <sub>max</sub> & R <sub>850</sub>	MSLP & Q <sub>850</sub> & T <sub>min</sub> & V <sub>850</sub>	MSLP & Q <sub>850</sub> & T <sub>min</sub> & U <sub>850</sub>
	Winter	T <sub>max</sub> & R <sub>925</sub>	T <sub>min</sub>	MSLP & Q <sub>850</sub> & T <sub>min</sub> & V <sub>850</sub>
	Spring	T <sub>max</sub> & R <sub>850</sub>	MSLP & Q <sub>850</sub>	MSLP & Q <sub>850</sub> & T <sub>850</sub>
<b>SEC</b>	Summer	T <sub>max</sub> & R <sub>925</sub>	MSLP & Q <sub>925</sub> & T <sub>min</sub>	MSLP & Q <sub>925</sub> & T <sub>min</sub>
	Autumn	T <sub>max</sub> & R <sub>925</sub>	MSLP & Q <sub>925</sub> & T <sub>min</sub>	MSLP & Q <sub>925</sub> & T <sub>min</sub>
	Winter	MSLP & T <sub>max</sub> & R <sub>925</sub>	MSLP & Q <sub>925</sub> & T <sub>min</sub>	MSLP & Q <sub>925</sub> & T <sub>min</sub>
	Spring	T <sub>max</sub> & R <sub>925</sub> & U <sub>850</sub>	MSLP & Q <sub>925</sub> & T <sub>min</sub>	MSLP & Q <sub>925</sub> & T <sub>min</sub>
<b>TAS</b>	Summer	MSLP & T <sub>850</sub> & R <sub>925</sub>	MSLP & Q <sub>850</sub>	MSLP & Q <sub>850</sub>
	Autumn	MSLP & T <sub>max</sub>	MSLP & Q <sub>925</sub>	MSLP & Q <sub>925</sub> & T <sub>min</sub>
	Winter	MSLP & T <sub>max</sub> & R <sub>925</sub>	T <sub>min</sub>	MSLP & Q <sub>850</sub> & T <sub>min</sub>
	Spring	MSLP & T <sub>max</sub> & R <sub>925</sub>	MSLP & Q <sub>925</sub> & T <sub>min</sub>	MSLP & Q <sub>925</sub> & T <sub>min</sub>

**Table 2b:** Optimum combination of parameters for each calendar season and the six regions for dT<sub>max</sub>, dT<sub>min</sub> and pE.

## 5) Evaluation of the SDMs used in the GUI

A careful evaluation of the skill of the SDM was carried out on different timescales: daily, inter-annual and long-term (see Appendix B for details). The technique was found to reproduce the main characteristics of the PDFs of local observed variables. In particular, the technique was found to be unbiased and it was able to reproduce the local means. However, like most statistical downscaling techniques, the analogue approach did not fully reproduce the observed variances of the series. That limitation occurred across all variables with a varying degree of severity. This drawback was found to be particularly important for rainfall: due to the non-normal distribution of daily rainfall, the reduction of variance leads to an underestimation of the mean (Timbal *et al.*, 2006). It was therefore decided to introduce a correction factor for rainfall applied to the reconstructed series and based on the local observed climate. It was done so as to reduce the underestimation of the variance and reproduce an unbiased mean. This correction was kept to a very simple level and is unchanged across all rainfall stations and seasons, in order to minimise the risk of over-fitting the SDM to the current climate.

It was shown that the technique overall was skilful at reproducing the observed PDFs for the right reasons. The daily variability is well reproduced, as captured by the day-to-day correlation between the observed and reconstructed series. In addition, the technique has skill in capturing inter-annual variability as well as long-term observed climatic trends.

For rainfall, it is notable that although the analogue approach is least skilful in terms of correlation (on both daily and inter-annual time-scale), it gives the most reliable reproduction of long-term trends of all predictands. This suggests that day-to-day variability of rainfall amount is largely affected by local effects not captured by large-scale variables. The large-scale variability and long-term trends, which remove a lot of this small temporal scale variability, is well tied to large-scale factors.

By contrast, the technique, while extremely skilful in reproducing temperature series on daily and inter-annual time-scales, seems to consistently underestimate (by a factor of two) the observed long-term warming. It was found that this underestimation is by and large due to the underestimation of the variance by the reconstructed series, leading to an underestimation of the magnitude of the trend.

For the newly developed moisture variables, the analogue technique performed relatively consistently with skill displayed across all statistics within the range of the two extremes provided by temperature and rainfall. It was noted, however, that for  $dT_{\min}$  the technique does not appear to reproduce much of the observed long-term trend, thus casting doubt on the ability of large-scale predictors to explain local trends for this variable; and hence suggesting that the method may not be able to provide meaningful downscaled projections for  $dT_{\min}$ .

The optimised SDMs were then applied to the CMIP3 climate models described in the next section. It is worth noting that the search for analogues is performed on normalised anomalies of the predictor fields. In the case of climate model simulations, normalised anomalies are calculated for the simulation of the 20<sup>th</sup> century, in effect removing model biases in the mean and variance reproduction of predictor fields. The model mean climatology is then used as a baseline to calculate anomalies for the predictors in future projections. This methodology assumes that the same model biases are affecting future projections and is commonly used in climate change science. Implicitly, this methodology corrects model biases both in the mean state and in daily variability; therefore the traditional evaluation of GCM performance in reproducing surface predictands as used in the Climate Change in Australia report (BoM and CSIRO, 2007) is not relevant here. However, all users should carefully evaluate the suitability of downscaled models for any impact study using the local predictands of interest generated by downscaling GCM simulations of the 20<sup>th</sup> century (20C3M).

It is worth remembering that the selection of the optimum combination of predictors is solely based on the observed past climate. The SDMs then rely on the hypothesis that the chosen predictors will capture the essence of the large-scale changes in a

future climate that will drive the local climate. This hypothesis has been investigated using discontinuities in our past climate records in specific cases discussed in the introduction. It will also be touched on during the evaluation of the skill of the model, in particular the ability of the SDMs to reproduce observed trends.

## 6) The Global Climate Models used in the GUI

Fully coupled Atmospheric and Oceanic General Circulation Models (GCMs), commonly referred to as global climate models, are complex numerical models which solve well established laws of physics, such as conservation of mass, energy and momentum of the components of the climate system. They include representations of the continental surface (hydrology, soil and vegetation) and of the cryosphere (land-ice, sea-ice and Polar Regions).

As part of the Intergovernmental Panel on Climate Change (IPCC) 4<sup>th</sup> Assessment of Climate Change Science released in 2007, a new set of coupled GCM experiments has been studied. This represents a major advance both for the evaluation of models and for the generation of climate projections. The open nature of output availability has resulted in this set of experiments being subjected to unprecedented levels of evaluation and analysis: the Coupled Model Intercomparison Project N°3 (CMIP3). The models represent the current state-of-the-art in climate modelling, with advances in sophistication in the physical parameterisations used, a greater number of components included and increased resolution in both ocean and atmosphere simulations. Model outputs were obtained from the IPCC Model Output website at [http://www-pcmdi.llnl.gov/ipcc/info\\_for\\_analysts.php](http://www-pcmdi.llnl.gov/ipcc/info_for_analysts.php).

Up to 23 GCMs contributed to the CMIP3 dataset; however only a subset of this database could be used because the SDM relies on daily outputs for the predictors. Therefore, GCMs are used only if the modelling group provided daily data for both the simulation of the 20<sup>th</sup> century and for simulations of the 21<sup>st</sup> century under different emissions scenarios. The models were ranked according to a measure of their sensitivity ( $\Delta T$ , last column in Table 3), calculated using the global warming produced by the model under the A1B scenario when approximated by linear regression over the 21<sup>st</sup> century (BOM and CSIRO, 2007). This measure helps the user to select models according to their global sensitivity.

Originating Group	Country	Acronym	Grid size (km)	$\Delta T$ ( $^{\circ}\text{C}$ )
CSIRO	Australia	CSIRO	~200	2.11
NASA/Goddard Institute for Space Studies	U.S.A.	GISSR	~400	2.12
Canadian Climate Centre	Canada	CCM	~300	2.47
Meteorological Research Institute	Japan	MRI	~300	2.52
Geophysical Fluid Dynamics Lab	U.S.A.	GFDL2	~300	2.53
Meteo-France	France	CNRM	~200	2.81
Geophysical Fluid Dynamics Lab	U.S.A.	GFDL1	~300	2.98
Institut Pierre Simon Laplace	France	IPSL	~300	3.19
Centre for Climate Research	Japan	MIROC	~300	3.35
Max Planck Institute for meteorology DKRZ	Germany	MPI	~200	3.69

**Table 3:** *Global climate models from the CMIP3 database to which the SDM was applied. The name and country of the originating group, the acronym used in the GUI and the approximate size of the model horizontal grid box are shown. Models are ranked according to a sensitivity measure (last column) from the least sensitive at the top to the most sensitive at the bottom.*

Future greenhouse gas and aerosol emissions due to human activities, such as energy generation, transport, agriculture, land-clearing, industrial processes and waste, are considered in the future scenarios. To provide a basis for estimating future climate change, the IPCC prepared a large range of greenhouse gas and sulphate aerosol emissions scenarios for the 21<sup>st</sup> century that combine a variety of assumptions about demographic, economic and technological driving forces likely to influence future emissions.

Up to six future emissions scenarios were used by the modelling groups that contributed to the CMIP3 database. Each emissions scenario leads to a different projected global warming range (Table 4). In order to reduce the amount of data used, only two scenarios for the 21<sup>st</sup> century have been downscaled: A2 and B1.

Scenario	Mean warming	Uncertainty range
<b>B1</b>	1.8°C	[1.1-2.9°C]
<b>A1T</b>	2.4°C	[1.4-3.8°C]
<b>B2</b>	2.4°C	[1.4-3.8°C]
<b>A1B</b>	2.8°C	[1.7-4.4°C]
<b>A2</b>	3.4°C	[2.0-5.4°C]
<b>A1FI</b>	4.0°C	[2.4-6.4°C]

**Table 4:** Mean global warming estimates for 2100, relative to 1990, for 6 emissions scenarios, derived from Figure SPM-3 of the IPCC (2007) report.

The A2 scenario is based on a very heterogeneous world with continuously increasing population and technologically fragmented economic development, leading to one of the highest emissions scenarios available. In contrast, in the B1 scenario the emphasis is on global solutions to economic, social and environmental sustainability, and B1 is one of the lowest emissions scenarios available. A simulation of the 20<sup>th</sup> century was also used, to complement the scenarios and provide a benchmark on the reliability of the downscaled GCMs.

Three experiments were therefore used for each GCM: a simulation of the 20<sup>th</sup> century (hereafter 20C3M) and two future projections for the 21<sup>st</sup> century using the two emissions scenarios mentioned above. The data available from the GCMs cover three time-slices for which daily DMOs were available and used by the GUI:

- 40 years from 1961 to 2000 for the 20C3M experiment;
- 20 years from 2046 to 2065 in the middle of the 21<sup>st</sup> experiments for both the A2 and B1 scenarios; and
- 20 years from 2081 to 2100 at the end of the 21<sup>st</sup> experiments for both the A2 and B1 scenarios.

## Part B: The Graphical User Interface

### 1) The software structure

#### f) Program flow chart

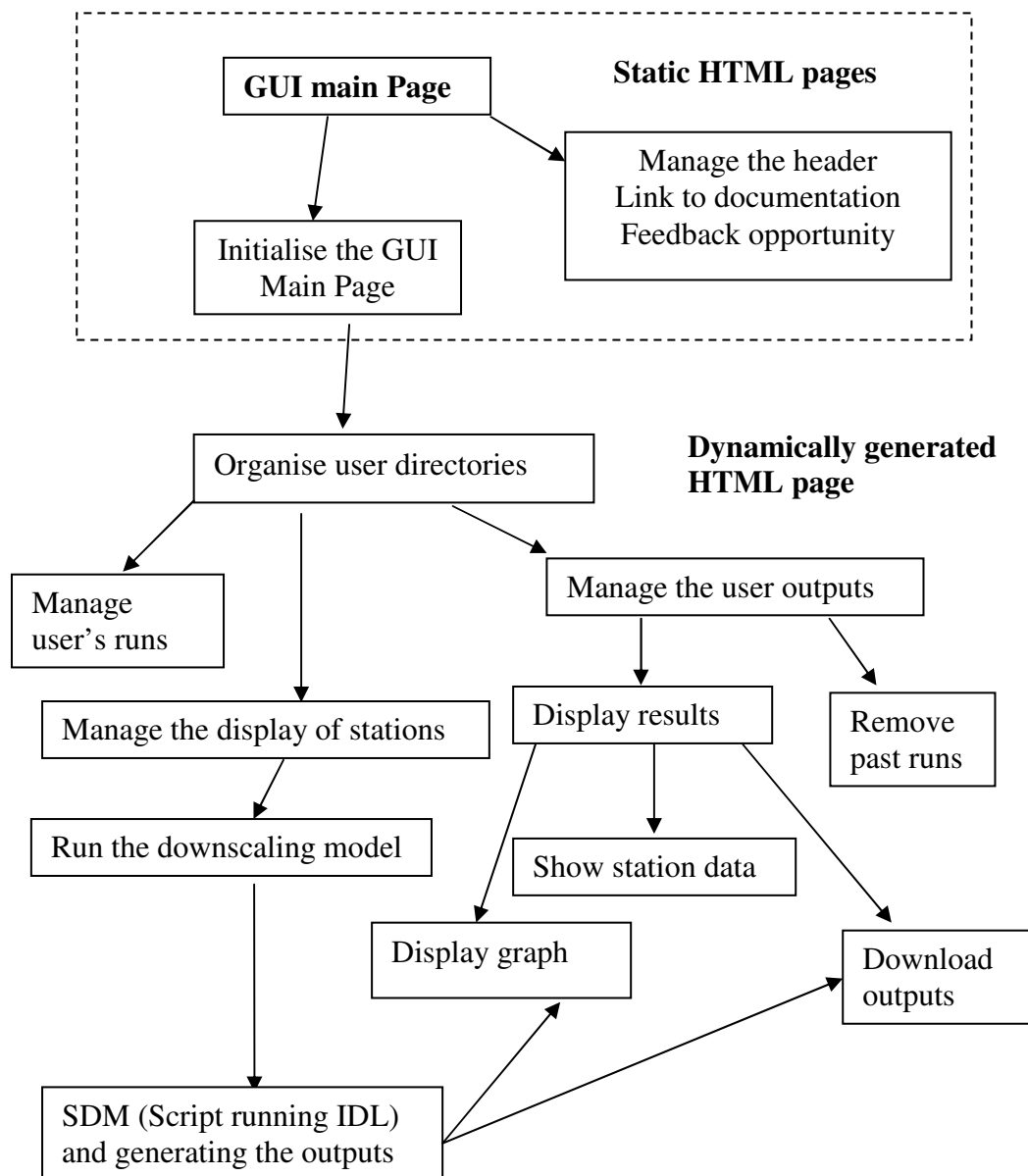


**Figure 3:** Architecture of the GUI for the Bureau of Meteorology SDM.

The GUI interface is constructed with four static HTML pages using JavaScript (Fig. 3). Additional pages and output datasets are generated dynamically using Perl in response to user inputs. The last component of the GUI is an Interactive Data Language (IDL) script which starts the calculation of the SDM itself. The entire SDM (data inputs, statistical calculation and visual outputs) is written in IDL. The SDM code can be run interactively in research mode; however, no access to the SDM code is given to the user through the GUI.

### **g) User management**

In order to run the SDM-GUI a temporary directory structure is created in the BOM computer system to store the results from the GUI. All individual user directories are treated as distinct sub-directories of a common root directory on a temporary disk space (*gwork*) on the Bureau's research machine *Gale* (more details on the user management and directory structure are provided in Appendix B). Due to IDL licensing limitations (IDL is a CPU intensive process with limited number of licences available); no more than three users are currently allowed to use the GUI simultaneously. If a fourth user tries to start a downscaling process, a warning will be issued indicating that the GUI has run out of licenses. The newcomer will have to wait until one of the current users quits the program.

Furthermore, each individual user directory is subdivided in sub-directories for each SDM run, allowing the user to perform and store the outputs of up to five downscaling experiments. Once this limit is reached, the user will need to remove an existing run in order to perform a new one.

Limited user information is kept in each user directory, including at what time the user started using the GUI. When returning to the GUI after a while, this time is checked to determine if the user should use an existing directory or get a new one. Currently, after 24 hours users lose their directory and its contents, making it available for new users.

## **h) Individual subroutines**

The static HTML pages and their usage are described in detail in the next section. A brief summary of the Perl scripts (\*.pl) and modules (\*.pm) is provided in Appendix C.

## 2) Using the GUI

### a) Access URL

Currently the GUI for the SDM runs on gale; the Bureau's research machine can only be accessed from within the Bureau's intranet and is not available on an external web site. However, access to the broader community on a dedicated web site supported by the Department of Climate Change (DCC) is being planned. The URL for access is:

[http://gale.ho.bom.gov.au/~bxt/sdm\\_gui.html](http://gale.ho.bom.gov.au/~bxt/sdm_gui.html)

*Note: Currently the GUI has only been tested and optimised for the Microsoft Internet Explorer web browser; problems will be encountered if users attempt to run the GUI with other browsers such as Firefox.*

### b) Front page layout

The front page layout (Fig. 4) has been kept to a minimum. It gives access to the available *documentation*: scientific literature underpinning the technical tool and the user manual -this document- including some technical description of the software and the IT choices made to optimise the usage.

The front page provides a button (*Contact*) for users to send feedback, comments or queries to the development team. In all subsequent pages, hitting the *Home* button will bring the user back to this front page. Hitting the *Start the GUI* button will lead the user to the interactive web interface itself.

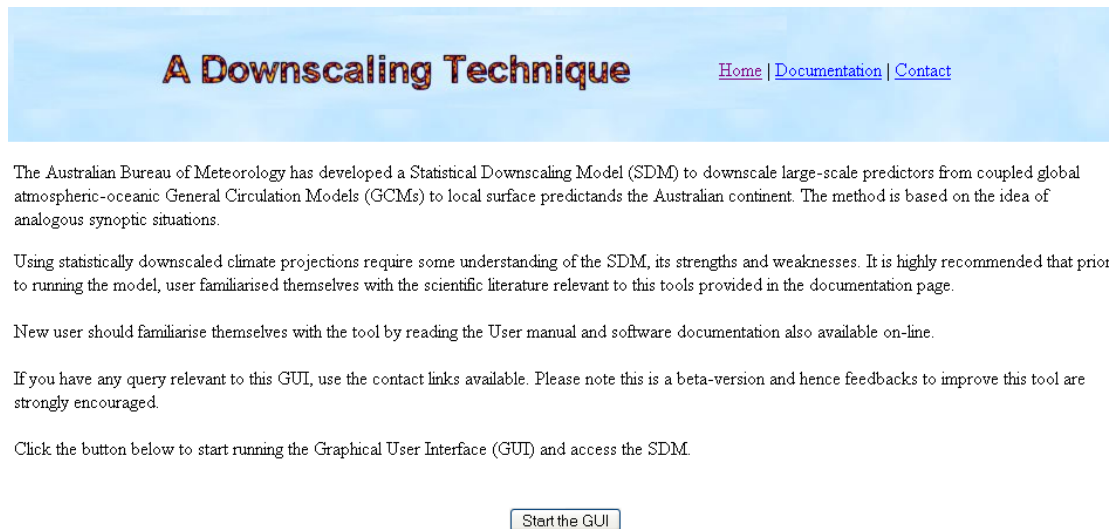


**Figure 4:** The front page of the GUI for the Bureau of Meteorology SDM.

### c) The interactive web interface

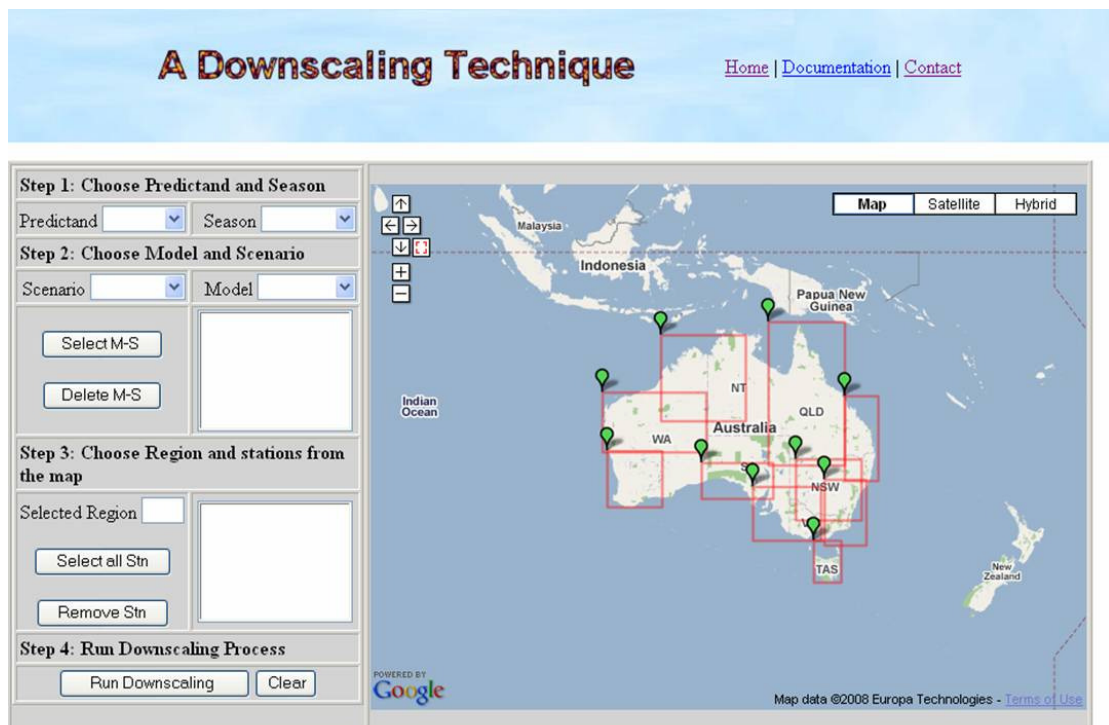


**Figure 5:** The default interactive GUI as it appears to the user before any action is taken.

The starting point of the GUI (Fig. 5) displays a large region around the Australian continent using MapData © powered by Google. It provides an option to choose the background between physical maps, satellite pictures or a combination of both (using the buttons displayed at the top right).

The user has a series of four steps to follow in order to carry out the downscaling process:

#### Step 1: Choose the predictand and season

- Select a predictand from the *Predictand* dropdown list: Rainfall,  $T_{\max}$ ,  $T_{\min}$ , pE,  $dT_{\max}$  and  $dT_{\min}$  (*Note: the extension of the GUI to pE,  $dT_{\max}$  and  $dT_{\min}$  is currently underway*)  
(*Note: it is possible to jump to step 3 following this selection and come down to the other steps later*);
- Select one of the calendar seasons from the *Season* dropdown list: Summer (December-January-February), Autumn (March-April-May), Winter (June-July-August), and Spring (September-October-November) (*Note: it is not possible at this stage to select several seasons, i.e. all year, in one go*).

#### Step 2: Choose the model(s) and a scenario

(*Note: it is not possible to combine the choice of model and the choice of scenarios, i.e. all simulations selected are based on a single choice of scenario*).

- Select the climate scenario from the *Scenario* dropdown list. Available scenarios are a simulation of the 20<sup>th</sup> Century (20C3M) providing daily data from 1961 to 2000, and future emissions scenarios A2 and B1 for the 21<sup>st</sup> century providing daily data for 20-year time slices: 2046-2065 for A2\_50 and B1\_50 and 2081-2100 for A2\_100 and B1\_100 (*Note: it is not possible at this stage to select several scenarios in one go*).
- Select the climate model(s) from the *Model* dropdown list. The user can choose all available models or select an individual CMIP3 model.
- Click the *Select M-S* button, a combination of model(s) and scenario will be added to the box below. All models can be selected in one go or individual

models one by one. By clicking on an individual model it can be removed from the list, using the *Delete M-S* button.

### Step 3: Select a region and the station(s)

*(Note: this step can actually be activated as soon as the predictand is chosen. Since the stations to be displayed depend on which HQ dataset is used, it does not require the other pull-down menus from step 1 and step 2 to be used).*

- Select the region of interest from the map. There are 10 available regions depicted as rectangular areas with a green marker on the upper left corner. When the mouse is over a green marker, a tool tip appears showing the abbreviation of the region name. Clicking on the green marker will display the region on the map and the *Selected Region* field will be filled with the abbreviation of the region. Fig. 6 shows an example for the Southwest of Western Australia (SWA) region.
- Select the stations. Available stations are displayed by yellow markers within the rectangular area. When the mouse is over a yellow marker, a tool tip shows the station name, and the latitude, longitude and height of the station. By clicking on the yellow marker, that station will be added to the text area next to the *Selected Region* field. At the same time, the yellow marker for this station will be removed from the map. To select all stations, click the *Select all Stn* button. To remove a selected station, highlight the station (multiple highlights allowed) and click the *Remove Stn* button. Removed stations will re-appear on the map as yellow markers.
- In some cases, a region is already selected but needs to be changed to another region. To make this change, click on the square shaped button next to the down arrow button on the map. This will lead back to the original display where the 6 regions are shown on the map.

### Step 4: Run the downscaling process

- Start the downscaling process by clicking on the button *Run Downscaling*.

- Clicking on the *Clear* button will remove all selected items and lead back to the start of the interface.

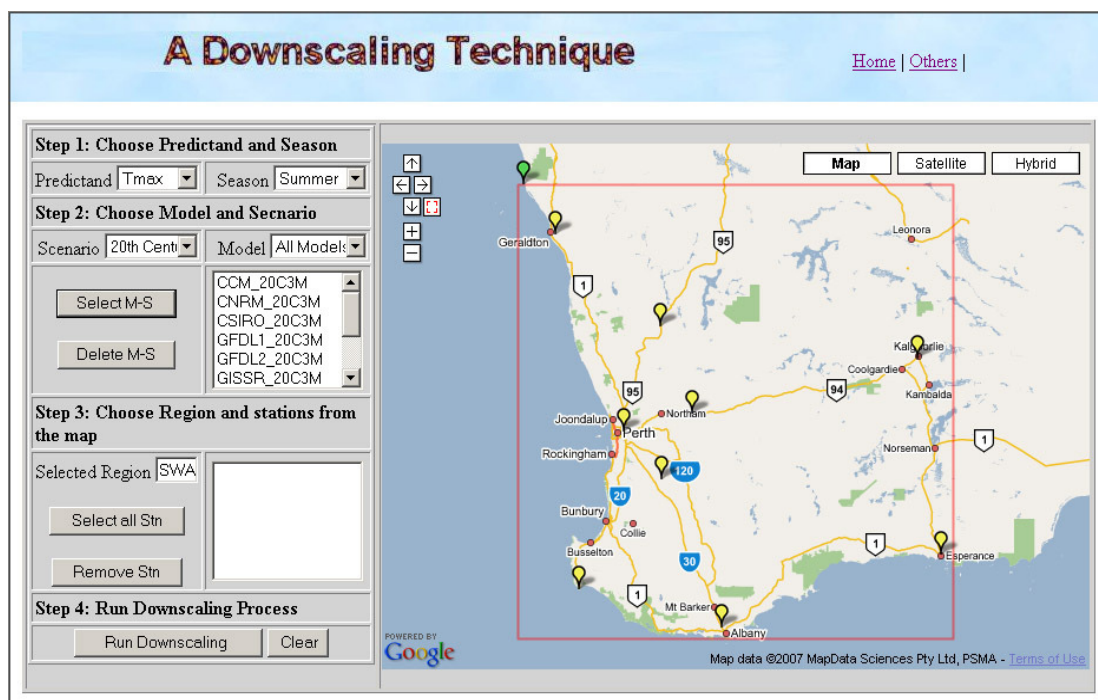


**Figure 6:** View of the GUI once a region (here, Southwest of Western Australia) and a predictand (here,  $T_{\max}$ ) have been selected.

Once the *Run Downscaling* button has been clicked, the GUI transfers the user's chosen options and runs the SDM IDL code on the Bureau machine Gale. Only a part of the entire SDM code is run on the fly to generate graphics and data output. It relies on intermediary files pre-calculated for all possible cases available via the GUI. These intermediary files are labelled *Change-Of-Date* (COD) files and contain the optimum analogue (i.e. a single best match) for any model day chosen within the 1958 to 2003 period in the NNR database (except from pan evaporation, for which data is restricted to the period 1975-2003). This optimal analogue depends on all the parameters chosen in the GUI: the predictand, the season, the region and the individual synoptic situation produced by the CMIP3 GCM. The downscaling process will take between one and two minutes to be completed, depending on the number of stations and the number of models being chosen.

### 3) Results provided by the GUI

#### a) Generating several outputs

Upon completion of the downscaling calculation, a table is generated and displayed underneath the user interface (Fig. 7).

## A Downscaling Technique

Home | Others |

Remove Stn

Capeleeuwin  
Cunderdin

Step 4: Run Downscaling Process

Run Downscaling
Clear



Map data ©2007 MapData Sciences Pty Ltd, PSMA - [Terms of Use](#)

Downscaling Output (User No. 1)

User/Run	Downscaling Options	Model-Scenarios and Stations	Results
1/1	Region: SEA Predictand: tmax Season: Summer	CCM_20C3M CNRM_20C3M CSIRO_20C3M GFDL1_20C3M GFDL2_20C3M GISSR_20C3M IPSL_20C3M MIROC_20C3M MPI_20C3M MRI_20C3M Portlincoln Snowtown Adelaide Nuriootpa Mountgambier Robe Nhill Melbourne Laverton Capeotway	<div style="margin-bottom: 5px;"><span>Show Results</span></div> <div><span>Delete This Run</span></div>
1/2	Region: SWA Predictand: rain Season: Summer	CCM_20C3M CNRM_20C3M CSIRO_20C3M GFDL1_20C3M GFDL2_20C3M GISSR_20C3M IPSL_20C3M MIROC_20C3M MPI_20C3M MRI_20C3M Kokardine Manarra Mingenew Perangery Willigulli Boyanup Capenaturaliste Caperiche Hopetoun Kendenup Kingriver Pardelup Peppermintgrove Wilgarup Cowcowing Cutting Doodardingwell Ejanding Meckering Merredin Nungarin Thegranites Trayning Walk_walkin Codg_codgen Arthurriver Broomehill Corrigin Cranbrook Nyerilup Theoaks Lakecarmody Menzies Norseman	<div style="margin-bottom: 5px;"><span>Show Results</span></div> <div><span>Delete This Run</span></div>

**Figure 7:** The GUI once two downscaling calculations have been performed. Both runs are summarised underneath the original interface which has been refreshed and is ready for a new simulation.

The first column of the table shows the assigned user number and the run number. The second column reminds the user of the downscaling options (predictand, season and region) selected for each individual run. The third column shows the model(s), scenario and station(s) selected. The fourth column allows two actions. One is to *Show Results*, discussed in the next section; the other is *Delete This Run*. This button allows the user to delete all outputs from a previous run and free space for additional runs.

Upon completion of the downscaling calculation, the GUI has been refreshed to the original (i.e. blank) state and is ready for an additional run (repeating steps 1 to 4). Results from follow-on simulations are shown in the Downscaling Output table alongside previous runs, but with a different run number (as in Fig. 7 after two runs).

*(Note: There is a limit of five runs kept on the machine at any time. Once five runs have been completed, the user will have to delete one of the earlier runs before being allowed additional runs).*

### **b) Graphics and Data Display and Download**

Clicking on the *Show Results* button in the Downscaling Output table opens a new browser window (Fig. 8), listing all figures and data files generated by this run. The number of outputs depends on the number of stations chosen. There is one data file (right box) per station, while graphical outputs (left box) are presented with eight individual stations per page. The number of graphical outputs vary with the predictand considered (graphical outputs are described in detail in Appendix F).

In order to display the data for a particular location, select the station file in the right box and click the *Show Data* button. A pop-up window will appear, containing the daily values for that location (Fig. 9). The number of columns depends on the number of GCMs chosen – one per model – plus a first column containing the date and a last column containing observations – either actual observations for the 20<sup>th</sup> century scenario, or *equivalent observations* from 1975 to 1994 for the 21<sup>st</sup> century scenarios (details are provided in Appendix F).

**Downscaling Output (User 1, Run 3)**

**Figures**

- m\_cpf\_rain1
- m\_cpf\_rain2
- m\_rain\_spell\_wsd1
- m\_rain\_spell\_wsd2
- m\_rain\_spell\_dsd1
- m\_rain\_spell\_dsd2
- intervar\_rain\_1
- intervar\_rain\_2

**Data**

- coondambo\_rain\_1a
- kondoolka\_rain\_1a
- nonning\_rain\_1a
- purple\_downs\_rain\_1a
- yardea\_rain\_1a
- farina\_rain\_1a
- marree\_rain\_1a
- pennalumba\_rain\_1a
- goode\_rain\_1a
- lakehamilton\_rain\_1a
- elliston\_rain\_1a
- nullarbor\_rain\_1a

[Download](#) all figures and data.

**Figure 8:** The outputs page showing all available outputs: figures (left box) and data files (right box). Upon a selection from either the list of figures or data files, it will be displayed in a pop-up window.

**mildura\_tmax\_1.data**

Date	CSIRO	MIROC	MPI	Observation
01012046	31.50	37.30	28.30	22.90
02012046	35.50	39.40	28.50	17.20
03012046	40.00	34.80	30.70	22.90
04012046	29.90	38.80	37.50	24.50
05012046	28.70	30.80	38.60	24.40
06012046	34.20	30.10	39.40	28.30
07012046	36.30	29.40	35.50	32.30
08012046	35.10	28.00	37.60	36.50
09012046	35.30	33.70	44.20	41.20
10012046	36.60	40.40	26.30	33.80
11012046	35.90	26.10	22.60	29.10
12012046	33.10	31.60	30.80	26.50
13012046	35.20	30.90	30.70	23.80
14012046	34.90	37.60	34.40	28.00
15012046	43.40	37.60	38.70	33.00
16012046	43.20	40.20	44.50	36.90
17012046	43.20	31.60	44.40	33.80
18012046	43.50	35.00	27.60	29.60
19012046	35.70	41.10	30.60	33.00
20012046	34.50	39.80	32.70	30.60
21012046	38.80	38.80	37.30	28.30
22012046	46.60	25.40	42.10	32.20
23012046	35.70	27.60	34.40	40.20
24012046	41.20	30.30	39.10	29.10
25012046	46.60	37.10	40.50	29.00
26012046	39.40	28.90	30.00	31.80
27012046	30.20	28.60	27.50	31.10
28012046	26.30	32.60	32.30	34.70
29012046	25.90	35.90	37.50	36.30
30012046	32.50	28.30	40.60	36.30
31012046	30.30	26.40	37.00	36.30
01022046	26.20	31.20	39.00	31.20
02022046	35.40	36.10	38.90	35.30
03022046	32.60	37.40	33.80	37.20
04022046	30.00	38.00	32.20	38.90
05022046	30.20	41.20	28.20	40.20
06022046	30.00	40.10	31.80	41.00
07022046	31.90	35.10	32.50	40.80

**Figure 9:** Tmax data for Mildura: the first column displays the dates, the subsequent ones (one column per model) show the projected downscaled value(s), and the last one displays the actual (or equivalent) observations for that day.

For a user to display a graph selected from the left box using the *Show Figure* button beneath the figure list, a package able to display postscript files would have to be available on the user machine (e.g. the freeware ghostview). Otherwise it is possible to download the files and print the figures on a postscript printer.

To download all figures and data, click on the *Download* link at the bottom of the page. A new browser window pops-up (Fig. 10), displaying three downloading options:

- ✓ figures as PostScript files; or
- ✓ figures in PNG format; or
- ✓ ASCII data files.

(Note: Since files are relatively small, all stations are bundled into one downloadable file).

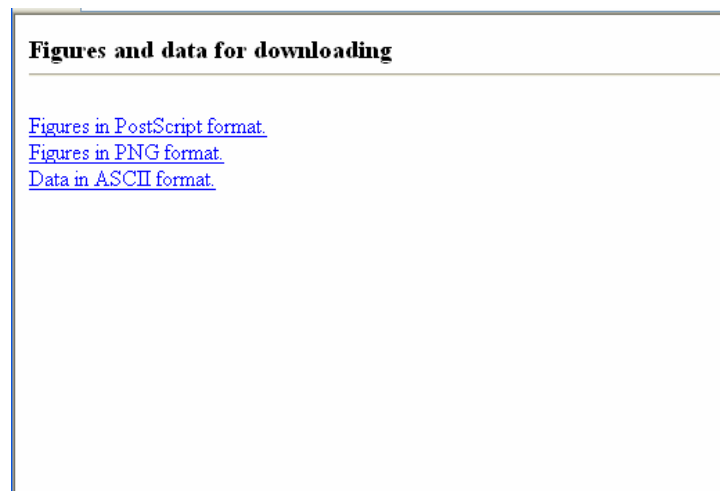


**Figure 10:** The download page showing available options to download outputs from a single run.

### c) Termination and closing

Upon completing all the simulations needed, the user should hit the *Close the GUI* button (and confirm that choice) rather than shut down the browser. This action will

delete all the data stored by the user and free space for a new user (this is important due to the licensing limitations mentioned earlier).

## 4) Summary and additional information

### a) Summary on the existing tool

The BoM statistical downscaling model, developed in earlier studies, has been generalised across half of the Australian continent. This method provides point-specific climate change projections relevant for impact studies across the continent in locations where high quality observations of the current climate are available. Individual SDMs were optimised using the high quality BoM network of observations for temperature (daily extremes:  $T_{\max}$  and  $T_{\min}$ ), rainfall, dew-point temperature (daily extremes:  $dT_{\max}$  and  $dT_{\min}$ ) and pan evaporation. Stations were lumped together into ten regional climate entities: five covering the southern part of the continent from the southwest of Western Australia to the east coast, one for the island of Tasmania and four covering the tropical northern part of the continent. For these last four regions, the SDM has only been optimised for temperature and rainfall. Each individual SDM was optimised in two steps: first the optimal combination of predictors was determined, and then additional parameters of the statistical model were determined (size of the domain from which predictors are obtained, calendar window and method to calculate daily anomalies). In total, 192 individual SDMs were optimised: six predictands times six regions (the southern half of Australia) plus three predictands times four regions (the tropical northern part of the continent), and in all cases for four seasons.

The analogue approach used here is one of the simplest existing downscaling methods. This allowed for the extensive work done calibrating the model. Despite its simplicity, this method has been shown to compare well with more advanced techniques (Zorita and von Storch, 1999). Simplicity, flexibility and robustness are essential to ensure that a single technique can be used across a range of variables and several climatic regions.

This is a landmark project, offering downscaled climate change projections across a large part of the Australian continent. It is worth noting that currently, downscaled predictands series are constructed independently from one variable to another. This is possibly a limitation for impact studies that require several predictands (i.e. rainfall and temperature).

### **b) Case studies performed with this tool**

A complete analysis of the outputs generated by the SDM-GUI is not viable; users are encouraged to generate outputs relevant to their particular location and application and to document results and possible issues arising from this exercise.

Nevertheless, some case studies have been documented in previous publications and are repeated in the appendices to illustrate the benefits and some known limitations from the downscaled projections:

1. Future projections for  $T_{\max}$  in Mildura (Victoria) are shown in Appendix G; this case was documented in Timbal *et al.* (2008a); and
2. Spatial heterogeneities within a typical model grid box for both temperature (along the NSW coast) and rainfall (in the southwest of Western Australia) are shown in Appendix H; these cases were documented in the Australian Climate Change report (BoM and CSIRO, 2007).

### **c) Future developments of the tool**

As noted earlier, currently downscaled predictand series are constructed independently from one variable to another. This is possibly a limitation for impact studies that require several predictands (i.e. rainfall and temperature). The possibility to generate multivariate projections and ensure full consistency between predictands will be investigated.

Further on-going developments are under way to maximise the benefits from this work. E.g., it is planned to provide gridded projections. The BoM has developed daily high resolution (0.05 by 0.05 degree) gridded data for rainfall and temperature (Jones *et al.*, 2007). This is an interesting development that could be used in the current framework to provide downscaled climate change projections on the same grid scale.

The adaptation of this synoptically driven technique to tropical areas has proven a challenging exercise. Results presented here show that the technique is less skilful in hot climate (e.g. summer and northern Australia), in particular for rainfall. It has also confirmed earlier findings that direct model outputs, such as rainfall, are more important in tropical areas to reproduce the local rainfall (Robertson *et al.*, 2004). In the course of this development it becomes apparent that improvements of the technique are needed to remove some of the issues described in this documentation. Therefore, the development of the BoM-GUI is likely to continue in the near future to ensure that it provides state-of-the-art downscale climate change projections.

Additional planned developments concern the web access to the GUI. Currently the GUI is only available internally within the BoM, and is used by regional climate service centres to provide tailored climate change projections upon request. The model is currently being ported on a national computing facility (the Australian Partnership for Advanced Computing, APAC) to provide a wider access for the research community. Furthermore, plans to provide outputs directly to the general public, as part of a larger online climate projections site (a central portal providing access to observed climate data and future projections generated by different methods – OzClim or the BoM SDM) are being investigated.

**d) Other existing software complementary to this tool**

The GUI has been developed specifically to be used within Australia and is particularly directed at impact studies (e.g. agriculture, health, ecology and economy). Currently most available tools rely on DMOs rather than downscaled projections: e.g. the Ozclim software (<http://www.csiro.au/ozclim/home.do>) developed by the CSIRO to provide regional projections across the Australian continent where various climate models information are interpolated on a high resolution grid (Ricketts and Page, 2007); or the TETYN software (<http://sourceforge.net/projects/tetyn/>) which used global database of climate indices (Solymosi et al., 2008). Besides tool based on DMOs, a few attempts have been made to enhance the relevance of the climate information provided by on-line software for high resolution impact studies by downscaling climate change information. The first documented attempt was the UK-based SDSM ([www.sdsm.org.uk](http://www.sdsm.org.uk)), this is a general downscaling methodology that one can optimise and applied anywhere once the local data needed are provided (Wilby et al., 2002); Hessami et al. (2008) described a regional optimisation and application for Canada. More similar in scope and method to the tool described here is the UK-based Environment agency Rainfall and Weather Impacts Generator, EARWIG however relies on a weather generator type of downscaling (Kilsby et al., 2008) as does RainSim (Burton et al., 2008) while the BoM-GUI, described here, relies on a physically-based downscaling method rather than a stochastic weather generator: namely meteorological analogues.

## Acknowledgements

The development of the Bureau of Meteorology (BoM) statistical downscaling technique has long been supported by the Department of Climate Change (DCC). The latest development of the graphical user interface was undertaken as part of the Australian Climate Change Science Program (ACCSP) and the support of the DCC. The extension of the technique to moisture variables was supported in part by the ACCSP and in part by the South-Eastern Australian Climate Initiative (SEACI). The predictand databases were obtained from the National Climate Centre (NCC) of the Bureau of Meteorology (BoM). NCEP/NCAR reanalyses were accessed from the Physical Sciences Division (PSD) of the Earth System Research Laboratory (ESRL), USA and processed by M. Collier (CSIRO) and P. Hope (BoM). We acknowledge the international modelling groups for providing their data for analysis, the Program for Climate Model Diagnosis and Intercomparison (PCMDI) for collecting and archiving the model data, the JSC/CLIVAR Working Group on Coupled Modelling (WGCM) and their Coupled Model Intercomparison Project (CMIP) and Climate Simulation Panel for organizing the model data analysis activity, and the IPCC WG1 TSU for technical support. The IPCC Data Archive at Lawrence Livermore National Laboratory is supported by the Office of Science, U.S. Department of Energy. Thanks are due to Aurel Moise and Lawson Mawson from the BoM for transferring the CMIP3 database to Australia. The authors wish to thank P. Wiles (Bureau of Meteorology, NSW regional office) and A. Roubicek (University of Macquarie, NSW) for their very useful suggestions in improving earlier versions of this document.

## Bibliography

- [1] Bureau of Meteorology and C.S.I.R.O., 2007: “Australian Regional Climate Change Projections”, AGO Technical report, 150 pp.
- [2] Burton, A., C. Kilsby, H. Fowler, P. Cowpertwait and P. O'Connell, 2008: RainSim: A spatial-temporal stochastic rainfall modelling system, *Env Model Software*, in press.
- [3] Charles, S., B. Bates, P. Whetton and J. Hughes, 1999: Validation of downscaling models for changed climate conditions: case study of southwestern Australia, *Clim Res*, 12, 1–14.
- [4] Charles, S., B. Bates and N. Viney, 2003: Linking atmospheric circulation to daily rainfall patterns across the Murrumbidgee River Basin, *Water Sci. Tech*, 48(7), 233– 240.
- [5] Christensen, J., B. Hewitson, A. Busuioc, A. Chen, X. Gao, R. Jones, R. Kolli, W.-T. Kwon, V. Magaña Rueda, L. Mearns, C. Meñendez, J. Raisanen, A. Rinke, A. Sarr and P. Whetton, 2007. In: *Climate Change 2007: The Physical Science Basis. Contribution of Working Group I to the Fourth Assessment Report of the Intergovernmental Panel on Climate Change*, chap. Chapter 11: Regional Climate Projections, Cambridge University Press, Cambridge, United Kingdom and New York, NY, USA.
- [6] Drosowsky W., 1993: An Analysis of Australian seasonal Rainfall anomalies: 1950-1987. I: Spatial Patterns. *Int. J. Climatology*, 13, 1–30.
- [7] Hessami, M., P. Gachon, T. Ouarda and A. St-Hilaire, 2008: Automated regression-based statistical downscaling tool, *Env Model Software*, 23(6), 813-834.

- [8] Hewitson, B. and R. Crane, 2006: Consensus between GCM climate change projections with empirical downscaling: Precipitation downscaling over South Africa, *Int J Climatol*, 26, 1315–1337.
- [9] Jones, D., W. Wang and R. Fawcett, 2007: Climate Data for the Australian Water Availability Project, Final milestone report, Bureau of Meteorology.
- [10] Jovanovic, B., D. A. Jones, and D. Collins, 2008: A High Quality Monthly Pan Evaporation Dataset for Australia. *Climatic Change*, published on-line.
- [11] Kalnay, E., M. Kanamitsu, R. Kistler, W. Collins, D. Deaven, J. Derber, L. Gandin, M. Iredell, S. Saha, G. White, J. Woollen, Y. Zhu, M. Chelliah, W. Ebisuzaki, W. Higgins, J. Janowiak, K. Mo, C. Ropelewski, J. Wang, A. Leetma, R. Reynolds, R. Jenne and D. Joseph, 1996: The NCEP/NCAR 40-year reanalysis project, *Bull Amer Meteor Soc*, 77, 437–471.
- [12] Kilsby, C., P. Jones, A. Burton, A. Ford, H. Fowler, C. Harpham, P. James, A. Smith and R. Wilby, 2007: A daily weather generator for use in climate change studies, *Env Model Software*, 22(12), 1705-1719.
- [13] Lavery, B., A. Kariko and N. Nicholls, 1992: A historical rainfall data set for Australia. *Aus. Met. Mag.*, 40: 33-39.
- [14] Lavery, B., G. Joungh and N. Nicholls, 1997: An extended high-quality historical rainfall dataset for Australia. *Aus. Met. Mag.*, 46: 27-38.
- [15] Lorenz, E., 1969: “Atmospheric Predictability as Revealed by Naturally Occurring Analogues”, *J. Atmos. Sci.*, 26, 636-646.
- [16] Lucas, C., 2006: A high-quality humidity database for Australia, in Proceedings of the 17<sup>th</sup> Australia New Zealand Climate Forum, p. p35, Canberra, Australia.

- [17]Ricketts, J. and C. Page, 2007: A web based version of OzClim for exploring climate change impacts and risks in the Australian region, in MODSIM07 proceedings, pp. 560–566.
- [18]Robertson, A., S. Kirshner and P. Smyth, 2004: Downscaling of daily rainfall occurrence over Northeast Brazil using a hidden Markov model, *J Climate*, 17, 4407–4424.
- [19]Solymosi, N., A. Kern, A. Maroti-Agots, L. Horvath and K. Erdelyi, 2008: TETYN: An easy to use tool for extracting climatic parameters from Tyndall data sets, *Env Model Software*, 23(7), 948-949.
- [20]Timbal B. and B.J. McAvaney, 2001: An Analogue based method to downscale surface air temperature: Application for Australia, *Clim. Dyn.* , 17, 947-963.
- [21]Timbal B., A. Dufour and B.J. McAvaney, 2003: An estimate of climate change for Western France using a statistical downscaling technique, *Clim. Dyn.*, 17, 947-963.
- [22]Timbal B., 2004: South West Australia past and future rainfall trends, *Clim. Res.*, 26(3), 233-249.
- [23]Timbal B., 2006a: Statistical Downscaling - an important part of ACCESS. In The Australian Community Climate and Earth System Simulator (ACCESS) - challenge and opportunities, *BMRC Research Report*, 123, 18th BMRC Modelling Workshop, pp 123-126.
- [24]Timbal B., 2006b: Statistical Downscaling in BMRC. In Climate change research in the Bureau of Meteorology, S.B. Power and K. Pearce (eds.), *BMRC Research Report*, 125, 68-72.
- [25]Timbal B. and J. Arblaster, 2006: Land covers change as an additional forcing to explain the rainfall decline in the South West of Australia. *Geo. Res. Let.*, 33, L07717, doi:10.1029/2005GL025361.

- [26]Timbal B., J. Arblaster and S. Power, 2006: Attribution of the late 20th century rainfall decline in South-West Australia. *J. Climate*, 19(10), 2046-2062.
- [27]Timbal, B. and D. Jones, 2008: Future projections of winter rainfall in southeast Australia using a statistical downscaling technique, *Clim Change*, 86, 165–187.
- [28]Timbal B., E. Fernandez and Z. Li, 2008a: Generalization of a statistical downscaling model to provide local climate change projections for Australia, *Environ. Soft. Model.*, doi:10.1016/j.envsoft.2008.07.007.
- [29]Timbal, B., P. Hope and S. Charles. 2008b: Evaluating the consistency between statistically downscaled and global dynamical model climate change projections, *J. Climate*, 21(22), 6052-6059.
- [30]Trewin, B.C., 2001: Extreme temperature events in Australia. PhD Thesis, School of Earth Sciences, University of Melbourne, Australia.
- [31]Uppala, S., P. Kallberg, A. Simmons, U. Andrae, V. da Costa Bechtold, M. Fiorino, J. Gibson, J. Haseler, A. Hernandez, G. Kelly, X. Li, K. Onogi, S. Saarinen, N. Sokka, R. Allan, E. Andersson, K. Arpe, M. Balmaseda, A. Beljaars, L. van de Berg, J. Bidlot, N. Bormann, S. Caires, F. Chevallier, A. Dethof, M. Dragosavac, M. Fisher, M. Fuentes, S. Hagemann, E. Holm, B. Hoskins, L. Isaksen, P. Janssen, R. Jenne, A. McNally, J.-F. Mahfouf, J.-J. Morcrette, N. Rayner, R. Saunders, P. Simon, A. Sterl, K. Trenberth, A. Untch, D. Vasiljevic, P. Viterbo, J. Woollen, 2005: The era-40 re-analysis, *Quart J Roy Meteor Soc*, 131, 2961–3012.
- [32]Van Den Dool, H., 1994: Searching for analogues, how long must we wait?, *Tellus*, 46A, 314-324.
- [33]Von Storch, H., 1999: On the Use of “Inflation” in Statistical Downscaling, *J Climate*, 12, 3505–3506.

- [34]Wilby, R., C. Dawson and E. Barrow, 2002: SDSM - a decision support tool for the assessment of regional climate change impacts, *Env Model Software*, 17, 145–157.
- [35]Wilby, R.L., S.P. Charles, E. Zorita, B. Timbal, P. Whetton and L.O. Mearns, 2004: Guidelines for Use of Climate Scenarios Developed from Statistical Downscaling Methods. Published on-line, supporting material to the Intergovernmental Panel on Climate Change, 27pp.
- [36]Zorita, E. and H. von Storch, 1999: The analog method as a simple statistical downscaling technique: comparison with more complicated methods, *J Climate*, 12, 2474–2489.

## Appendix A: Analysis of the SDM optimised parameters

Statistics on the type of predictors chosen reveal that the best combinations are based on temperature, air flow, moisture and synoptic predictors. The optimal number of predictors within a combination (Fig. A1) is often three (apart from pan evaporation where most frequently only two predictors are used). When a different number of predictors are required for the optimum combination, it is often less than three predictors apart from rainfall. The need for a large number of predictors for rainfall shows that it is a difficult predictand to capture from large-scale analogues. Not only does rainfall require a large number of atmospheric variables, but it is the predictand for which skill scores are the lowest (see details in the next section). There are a few cases for each predictand (except for pE) where no combinations of predictors were found to improve on the best performing single predictor.

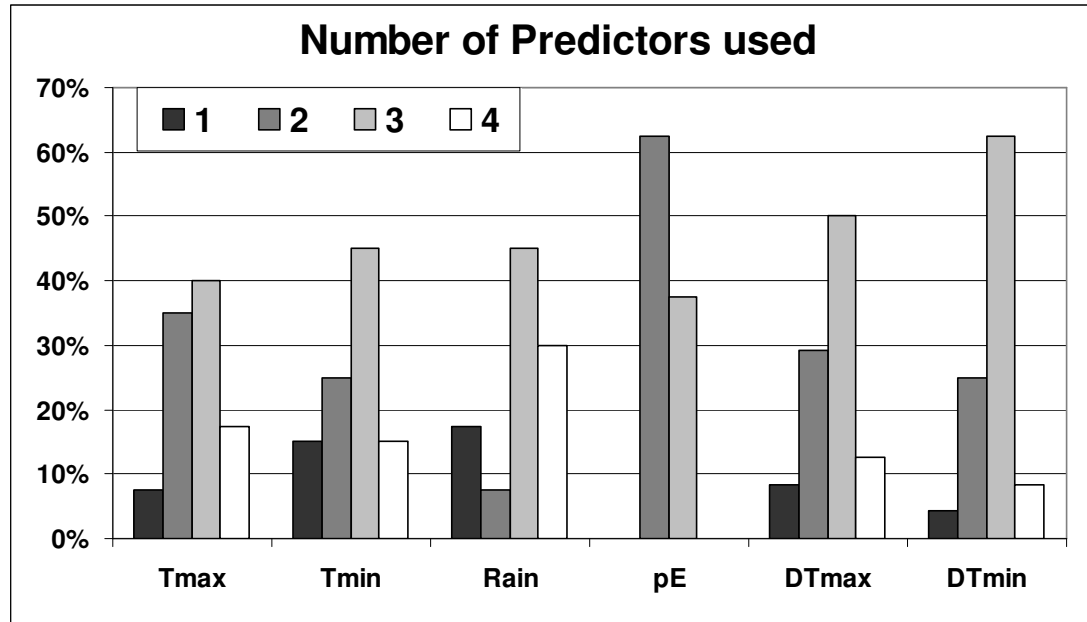


**Figure A1:** Number of predictors used (in percentage) over all SDMs for every predictand.

Mean sea level pressure (MSLP) is the most frequently chosen predictor (Fig. A2, top left). It is used for most individual SDMs in the case of rainfall,  $dT_{\max}$  and

dTmin but is picked up far less often for pan evaporation. This feature, combined with the fact that the SDM shows overall low skill (discussed in the next section) for pan evaporation, suggests that MSLP is a critical predictor for a synoptically-driven technique such as the analogue approach; when it does not perform as a useful predictor, none of the other available predictors can compensate for the lack of skill contribution from MSLP.

To predict rainfall in the tropical half of Australia, MSLP combined with Z500 (geopotential height at 500hPa) adds extra skill to the model. Unfortunately, Z500 is not available in the CMIP3 datasets so the SDM has been downgraded for these regions to less skilful models using only variables stored from the IPCC models runs.

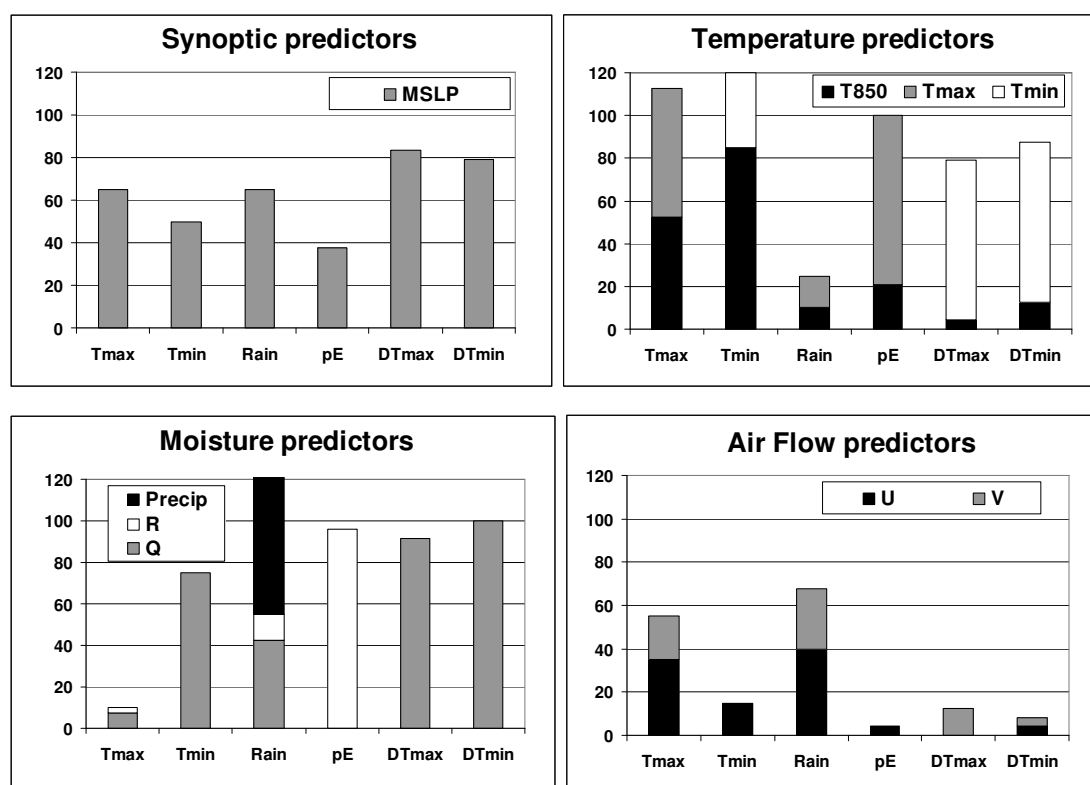


**Figure A2:** Percentage of SDMs where a particular type of variable is part of the optimal combination of predictors: synoptic predictors (top left), moisture predictors (bottom left), temperature variables (top right) and air flow predictors (bottom right) for the individual SDMs separated according to the predictands being modelled. For Tmax, Tmin and Rain, each bars based on 40 cases: ten regions times four seasons; for pE, DTmax and DTmin, each bar is only based on 24 cases: six regions times four seasons.

Thermal predictors (Fig. A2, top right) are very important, especially for  $T_{\max}$  and  $T_{\min}$ . In general,  $T_{850}$  is the most important thermal predictor, although  $T_{\min}$  is more important for  $dT_{\min}$  and  $dT_{\max}$ . Dew-point temperature, in most instances, has a weak diurnal cycle with maximum values in the early morning and maximal value in the afternoon (Lucas, 2006). Therefore, while the importance of  $T_{\min}$  for  $dT_{\max}$  is logical, its relevance for  $dT_{\min}$  is less intuitive. A total percentage in excess of 100% means that in some cases more than one thermal predictor is used in the optimised combination. The additional predictor is usually  $T_{\max}$  for  $T_{\max}$  and  $T_{\min}$  for  $T_{\min}$ , a clear indication that in these cases lower tropospheric temperature alone is not a sufficient predictor. In these rare occurrences, with two very similar and highly correlated predictors being used, the risk of over-fitting the SDM exists. However, in these instances it was found that the gain in skill for the SDM warranted this choice. Finally, thermal predictors rarely matter for rainfall to reproduce current climate; however, their importance in a future warmer world remains possible. E.g. it was found while comparing analogue-base projections for rainfall in the South-West of Western Australia with direct model outputs and another SDM, that the inclusion of  $T_{850}$  was necessary to have consistent projections between the three approaches (Timbal *et al.*, 2008).

Moisture variables (Fig. A2, bottom left) are also important as predictors across all predictands with the notable exception of  $T_{\max}$ . Specific humidity is almost always picked up apart from pan evaporation for which relative humidity is more skilful. Rainfall is often part of the optimised predictor's combination to downscale rainfall. As for temperature, there are instances (about 20% of the cases) where it is used in combination with another low level tropospheric moisture fields, suggesting a possible over-fitting.

Finally, some measure of the air flow (either the zonal ( $u$ ) or meridional ( $v$ ) component of the wind) is often added to the optimised combination (Fig. A2, bottom left). The fact that it is an additional predictor to the de-facto combination of synoptic-thermal-moisture is evident from examining Tables 2a and b. It is most useful for rainfall and  $T_{\max}$ , and least useful for dew-point temperature and pan evaporation. The zonal component is the most frequently used.

Overall statistics on the choice of the three additional parameters optimised for each individual SDM show some patterns worth commenting. The optimum size of the geographical domain used to search for analogues (the small domains are shown in Fig. A3a and large domains in Fig. A3b) is most often the larger of the two sizes tested (Fig. A4). There is a hint that the need to reduce the size of the geographical domain is seasonally dependent, with the use of the smaller domain being more frequent during the warmer seasons (40% of all SDMs in summer and 54% in autumn, compared to 40% and 38% in winter and spring).

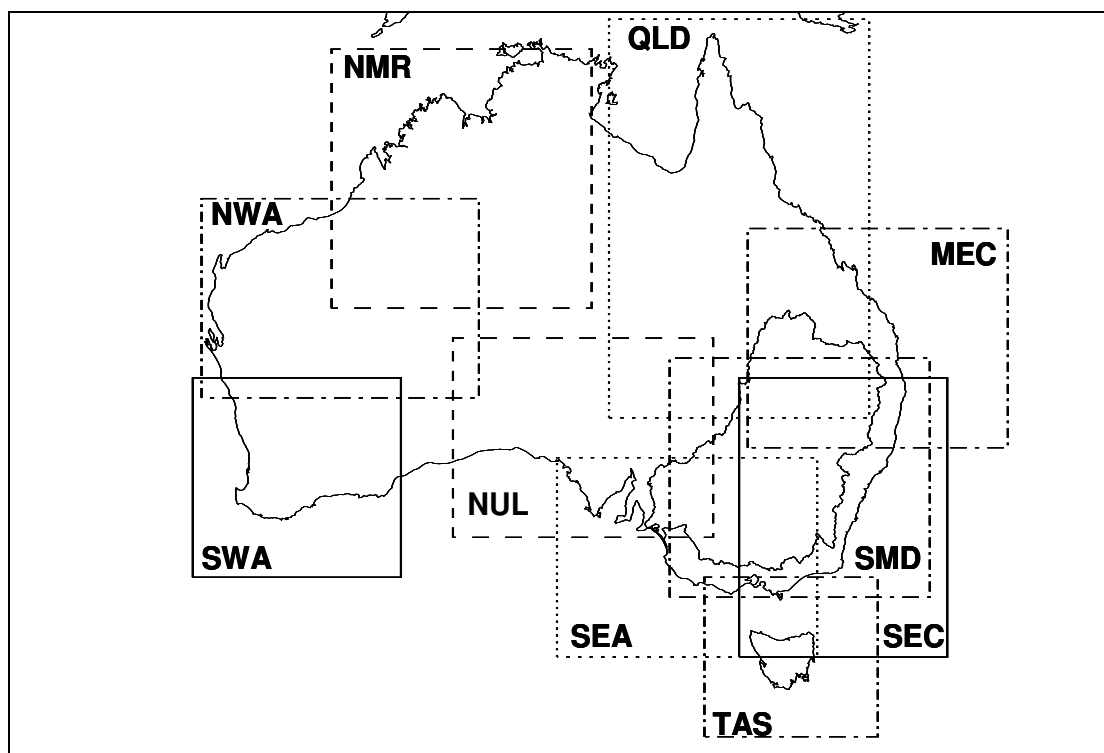


**Figure A3a:** *Small Geographical domains on which the predictors are used for the six areas of interest (SWA: solid line, NUL: dashed, SEA: dotted, SMD: dash-dotted, SEC: solid line, TAS: dash-dotted, NWA: dash-dotted, NMR: dashed, QLD: dotted, and MEC: dash-dotted).*

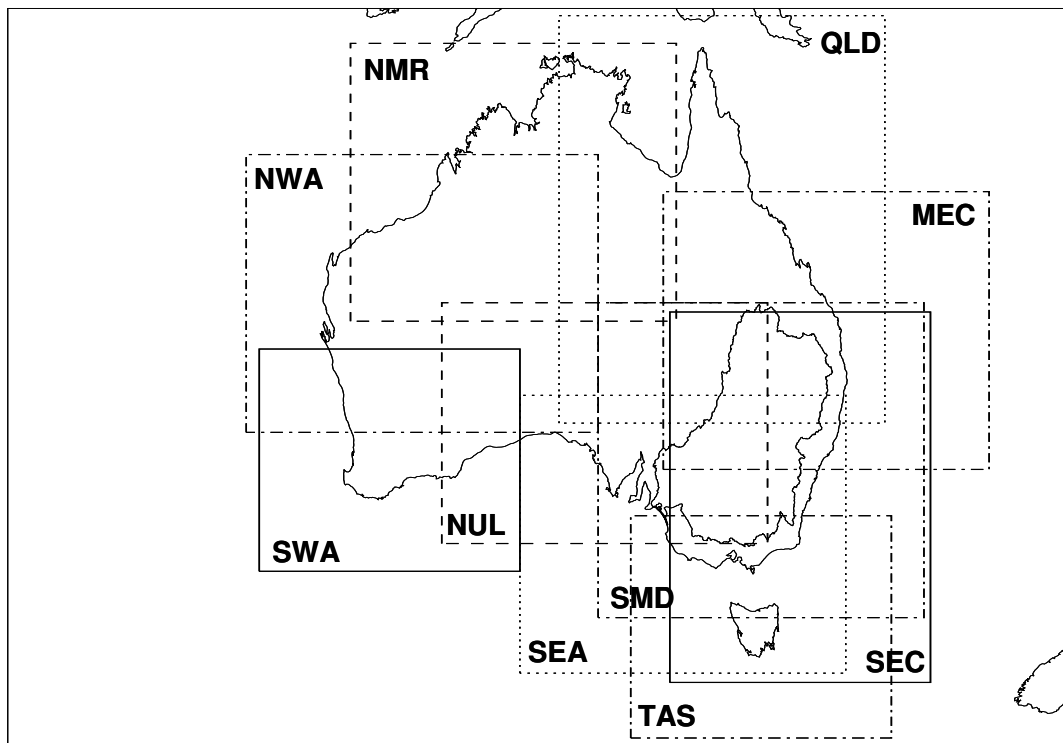


**Figure A3b:** Large Geographical domains on which the predictors are used for the six areas of interest (SWA: solid line; NUL: dashed, SEA: dotted, SMD: dash-dotted, SEC: solid line, TAS: dash-dotted, NWA: dash-dotted, NMR: dashed, QLD: dotted, and MEC: dash-dotted).

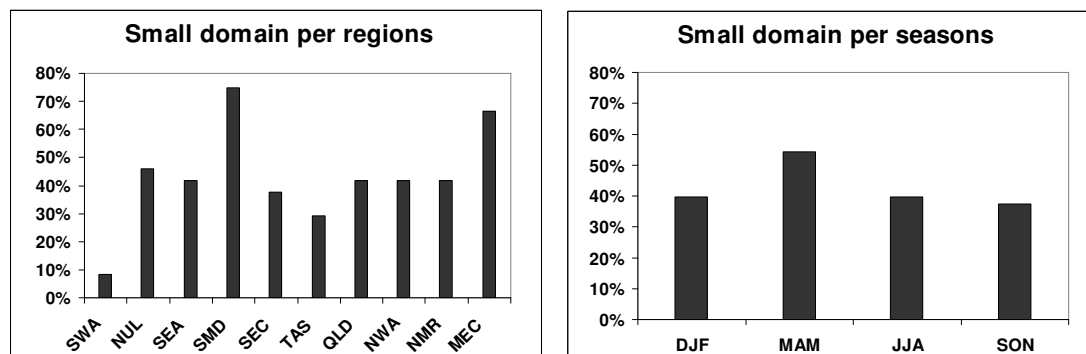


**Figure A4:** Percentage of cases in which the smaller geographical window is the best domain to search for analogues. Two sizes were tested for each SDM.

However, the most important factor appears to be the dependence on the region. Although the original two sizes tested for each region were chosen carefully based on rules derived from previous studies, regarding size and position (Timbal and

McAvaney, 2001), there were cases (such as SWA) where the small domain was too small and hence seldom chosen (only 8% of the time); whereas in SMD, the small domain was chosen 75% of the time, and between 29 and 67% in the other regions.

The choice between monthly and seasonal anomalies reveals a marked preference for using a single seasonal mean (Fig. A5, left), in particular for the transitional seasons (autumn 92% and spring 88% of all cases). This result was expected, as the underlying assumption behind using monthly mean is to reduce the non-stationarity across the months when calculating the anomalies, hence reducing the importance of the annual cycle when choosing an analogue. This result is particularly marked for temperature (95% of all SDMs for  $T_{\max}$  and 90% for  $T_{\min}$ ) and less for rainfall (65%) as expected since the annual cycle is more pronounced for temperature than for rainfall (Fig. A5, right).

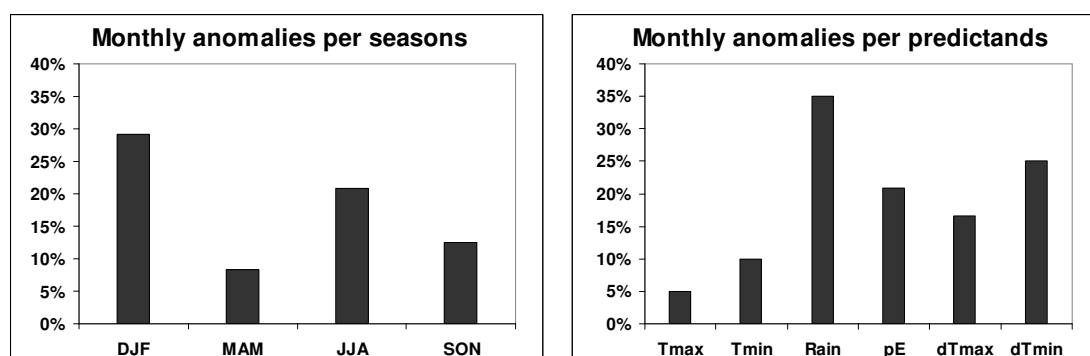


**Figure A5:** Percentage of cases for which monthly anomalies are chosen instead of anomalies based on seasonal means.

Finally, the calendar window (dTcal) was tested (Fig. A6). This is the number of days before and after the calendar dates which are used to find an analogue. For example, when searching for an analogue for the 1<sup>st</sup> of July:

1. if dTcal=15 then analogues can only be chosen between the 16<sup>th</sup> of June and the 16<sup>th</sup> of July;
2. if dTcal=30, analogues are chosen between the 1<sup>st</sup> of June and the 31<sup>st</sup> of July; and

3. if  $dT_{cal}=60$ , analogues are chosen between the 1<sup>st</sup> of June (this remains unchanged as analogues are only searched for within the same calendar season) and the 30<sup>th</sup> of August.

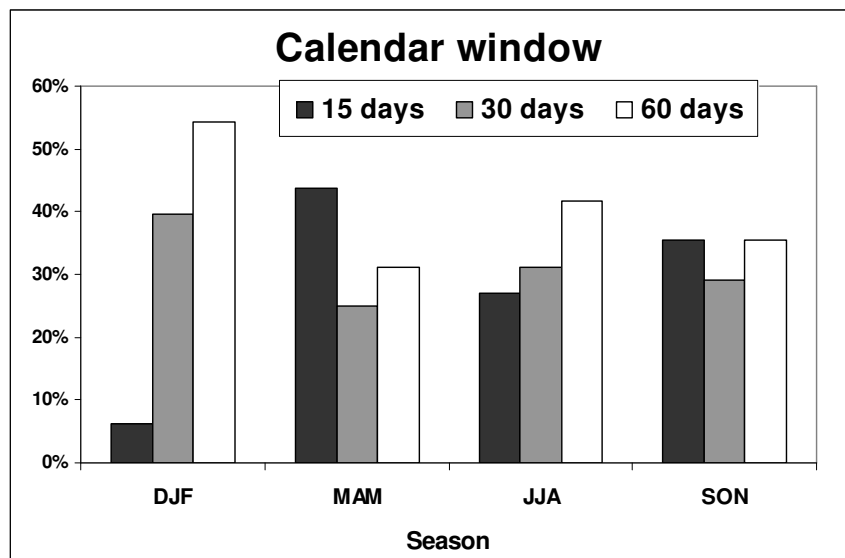


**Figure A6:** Optimum size of the calendar window (15, 30 or 60 days) as a function of the season of the year.

The limitation to search for an analogue only during the same calendar season is arbitrary but responds to the fact that large-scale meteorological forcings of the local climate change seasonally, during the year (as reflected in the optimum combination of predictors discussed earlier). Accordingly, the size of the calendar window is used to force the choice of analogue during the same part of the season. However, a bigger value for the calendar window would provide a potentially larger pool of analogues; hence the choice of the calendar window is a trade-off between these two effects. As expected, there is tendency to choose a smaller calendar window for the transient seasons (spring and autumn), when the underlying stationarity assumption is less true; and a tendency to choose a larger calendar window in winter and in particular in summer, when the size of the pool of analogues is most important.

## Appendix B: Analysis of the SDM skill

The skill of the SDM was evaluated using a range of metrics on different time scales. First, the ability of the technique to reproduce the observed Probability Density Functions (PDFs) was evaluated by looking at the first two moments of the PDFs: the mean and the variance.

The reproduction of the mean values for each predictand (Fig. B1) is very accurate. On each graph, each point corresponds to a single location for a single season, with the observed mean value on the x-axis and the reconstructed mean along the y-axis. The number of points in each graph is equal to the total number of stations captured in one of the ten climate regions (only six regions for dTmin, dTmax and pE) times four (between 1012 for rainfall and 76 for dew-point temperature). A perfect match would see all the points aligned with the diagonal. For most predictands, errors in the reproduction of the mean are relatively small and there is no clear evidence that the SDMs have a bias toward higher or lower values. Furthermore, there is no evidence that the SDMs have more difficulties in reproducing observations at either side of the spectrum (minimum or maximum values).

Similarly, results are shown for the reproduction of the variance (Fig. B2). It is clear that the technique has a tendency to underestimate the observed variance (points are aligned below the diagonal) for all variables. This is a known problem of statistical downscaling techniques (van Storch, 1999), and although the analogue approach is less affected than many other techniques (in particular linear techniques), it remains an issue.

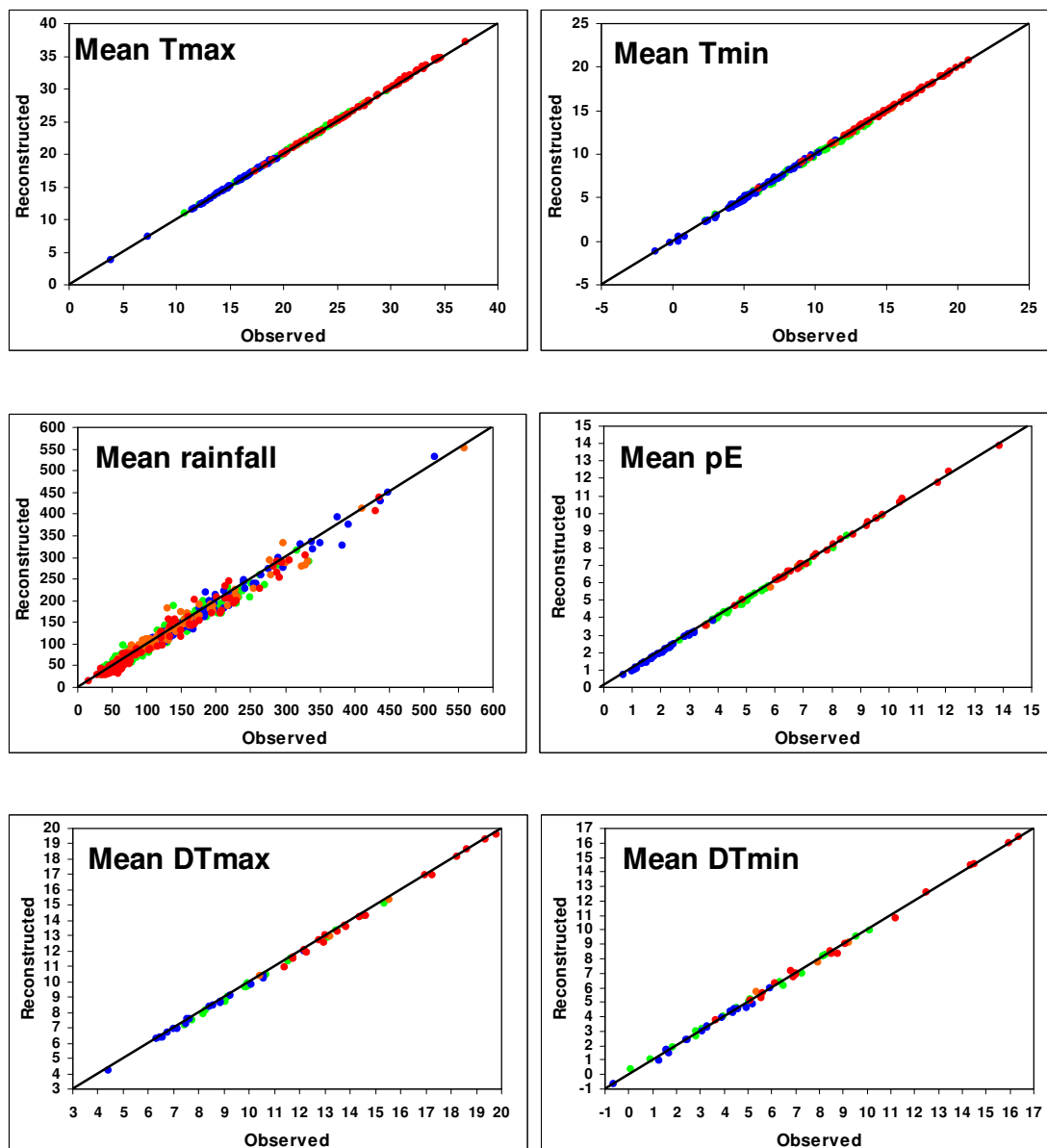


**Figure B1:** Scatter plot of the reconstructed versus observed means of the series for the six predictands. On each graph, there is one point per station and per season. The total number of points per graph is the number of stations across the ten regions times four for Tmin, Tmax and Rain; the six regions times four for dTmin, dTmax and Evap. The line of perfect fit (the diagonal) is shown. The colour code refers to the season: blue is winter, green is spring, red is summer and orange is autumn. Units are °C for temperatures and dew-point temperatures, mm for rainfall and  $\text{mm day}^{-1}$  for pan evaporation.

In the case of rainfall, it is worth noting that the reproduction of the mean is dependent on the ability of the technique to reproduce the observed variance, because rainfall is not normally distributed. In the case of the other variables, as daily values

are more normally distributed, the underestimation of the variance does not have a flow on effect on the reproduction of the mean.

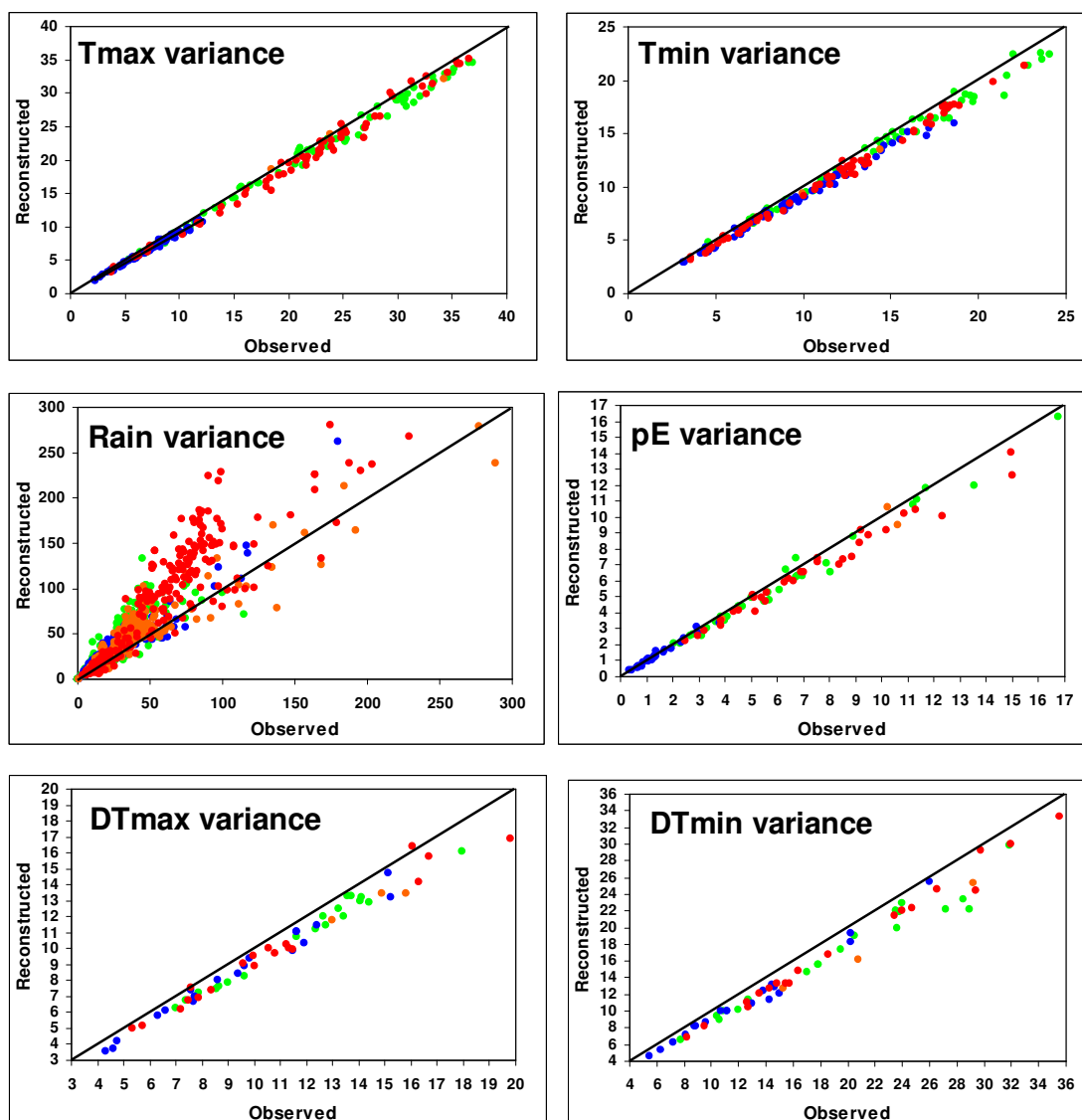


**Figure B2:** As per Figure B1 but for standard deviations (same units as for the means).

For this reason, Timbal *et al.* (2006) introduced a correction factor to adjust the reconstructed rainfall series, enhance the variance and improve the reproduction of the mean. The rationale for the correction applied is that the reconstructed rainfall is affected by the size of the pool of analogues to choose from; therefore in the case of large rainfall events, which are rare, the error is larger. The size of the pool depends on the ratio of rain days over dry days. It was decided that a very simple factor should be applied to limit some of the danger linked to artificially-enhanced variances

in downscaling techniques (van Storch, 1999). Therefore a single factor was used, which only depends on the availability of dry and wet days to find a suitable analogue across all stations and all seasons:

$$C_{factor} = 1 + 0.1 \times \frac{N_{dry}}{N_{wet}} \quad \text{and} \quad C_{factor} \leq 1.5$$

Where  $N_{dry}$  and  $N_{wet}$  are the number of dry and wet ( $> 0.3\text{mm}$ ) days observed for the season at an individual location. Note that all rainfall results presented so far include this factor, showing the ability of this simple correction to return unbiased mean rainfall estimates (Fig. B1) and very low rainfall variance biases compared to the other predictands, for which no attempt has been made to enhance the daily variability (Fig. B2).

Besides the ability of the technique to reproduce the observed shape of the PDFs as defined by the first two moments of the series, it is important to ensure that the technique is skilful in reproducing day-to-day variability that is driven by large-scale synoptic changes. A random choice of analogue may reproduce perfectly the observed mean and variance but may not be a skilful model. The Pearson correlation between daily observed and reconstructed series was calculated separately per region, per season and for each predictand. Each number is an average across all observations available in each region (Fig. B3). The results show a contrast between predictands; the SDM appears to be more successful for  $T_{max}$ ,  $T_{min}$  and  $dT_{max}$  than for pan evaporation and  $dT_{min}$ . For rainfall, correlations are by far the lowest, although due to the very large sample considered (about 4500 days), all these correlations are significant at least at the 95% level (based on rain occurrences only in the case of rainfall), indicating some level of skill. For most variables there is a marked seasonal cycle in skill, consistent across all regions, i.e. the analogue approach is particularly successful in autumn and spring for temperature predictands  $T_{max}$  and  $T_{min}$  (nearly reaching a correlation of 0.9 for  $T_{max}$  in autumn in several regions) and for pan evaporation (albeit with lower values). For rainfall, although correlations are low across all seasons, they peak in winter (between 0.3 and 0.4) apart from QLD region where the correlation is below 0.2 in all seasons and NMR region where the peak is in spring. For dew-point, seasonal variations of the results are less marked and not consistent across regions. Finally, there seems to be a high consistency in the

performance of the SDMs across the ten regions considered. Overall no particular region stands out as a climatic entity where the SDM skill in reproducing day-to-day variability is consistently lower or higher across all variables and seasons. The fact that the model was assumed to be applicable in all the extra-tropical regions of the Australian continent, where the climate is driven by synoptic disturbances, is vindicated by these results.

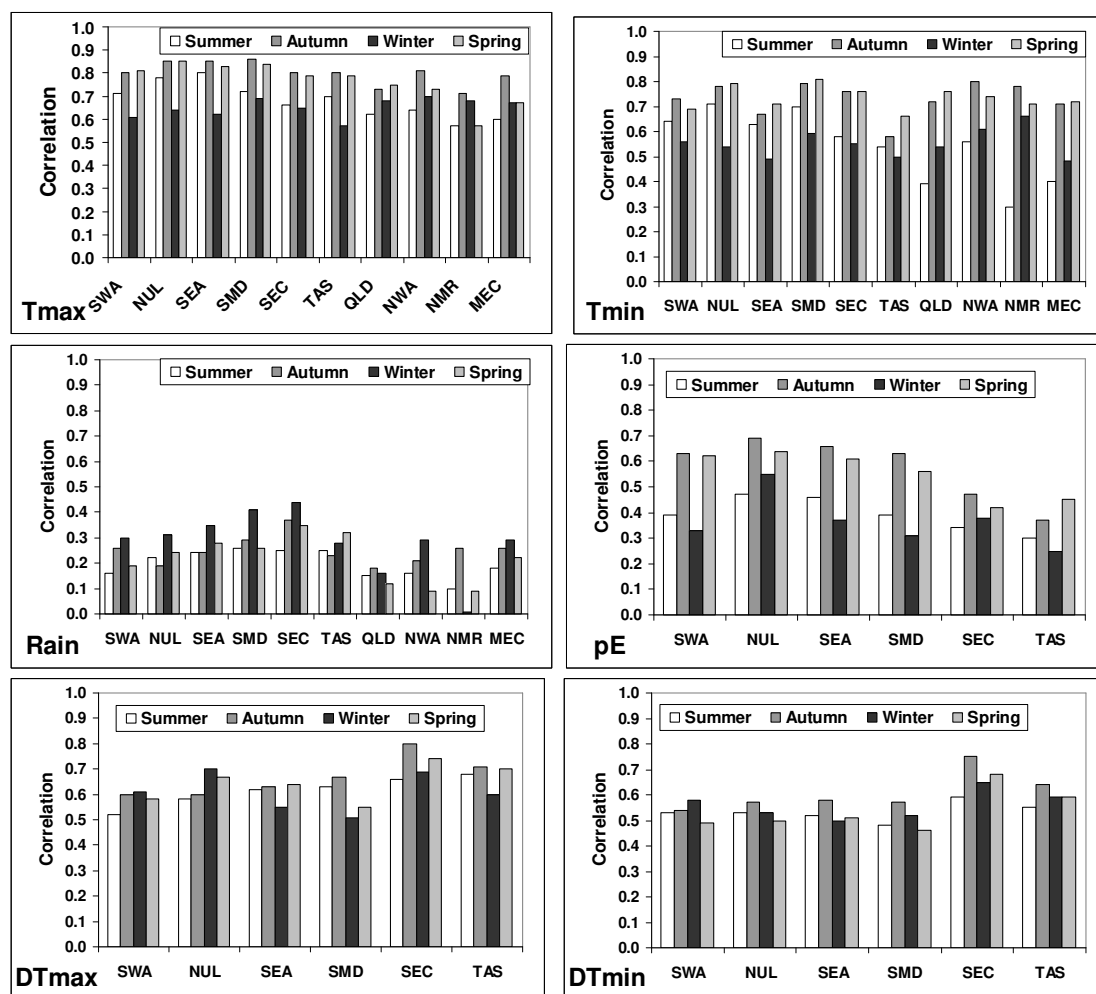


**Figure B3:** Correlation between daily observed and reconstructed series separated by season (different coloured bars) and region (names on the x-axis) for the six predictands considered (names at the bottom left corner). Each value is the average correlation across all the stations available in a particular region. For T<sub>min</sub>, T<sub>max</sub> and Rain, 10 regions are available; only the 6 covering the southern half of the continent are available for pE, dT<sub>min</sub> and dT<sub>max</sub>.

The ability of the modelled series to reproduce year-to-year variability is also important in a climate change context. It is evaluated by computing the Pearson correlation between seasonal means of the observed and reconstructed series (Fig. B4),

in the same way as daily variability. The length of the observed record is 1958 to 2003 for all predictands except for pan evaporation for which it is 1975 to 2003.

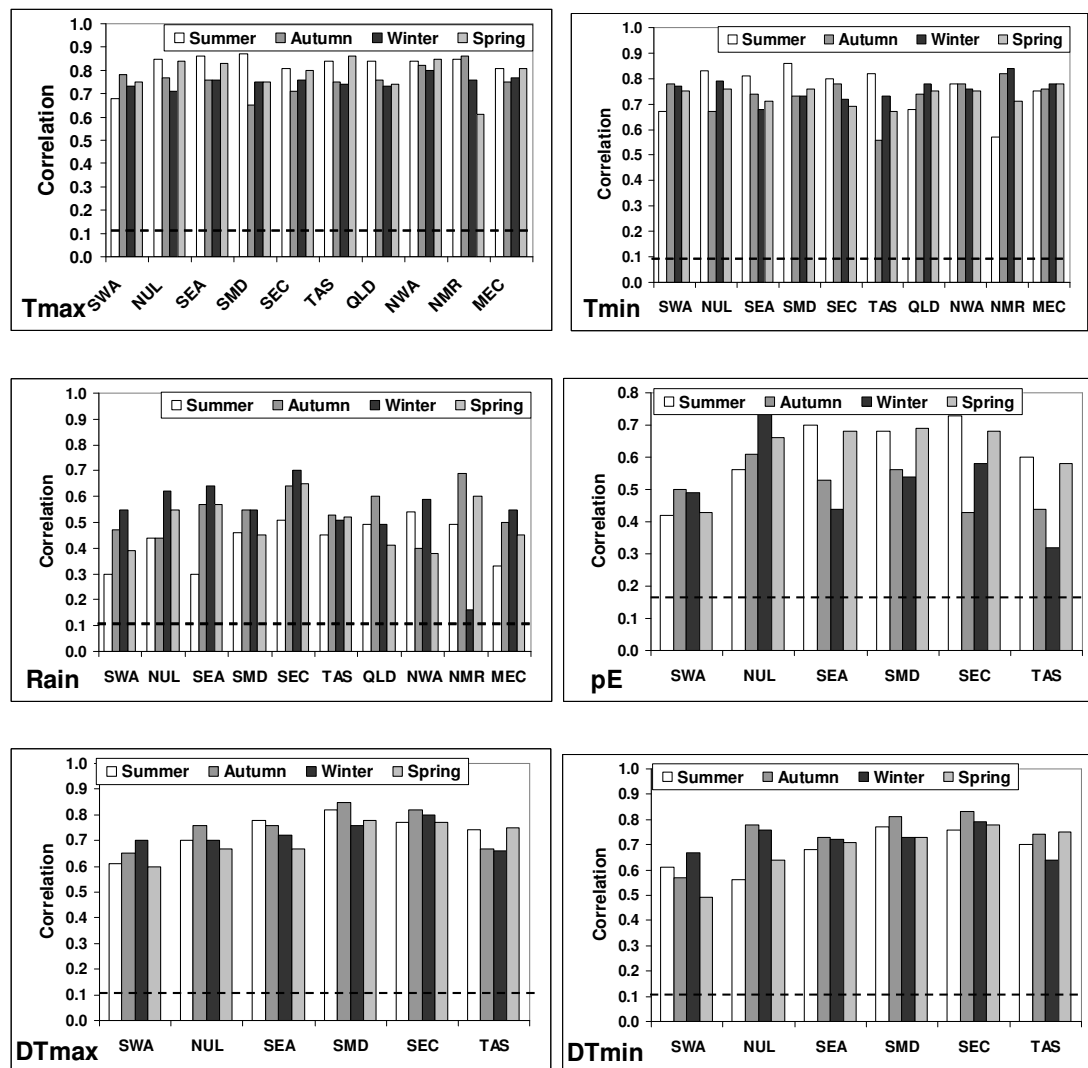


**Fig B4:** As per Figure B3 but for seasonal means. In addition, the dashed lines indicate the 95% confidence level for these correlations.

The percentage of observed inter-annual range (i.e. the difference between the highest and lowest seasonal totals in the observed record) reproduced by the reconstructed series is also evaluated (Fig. B5).

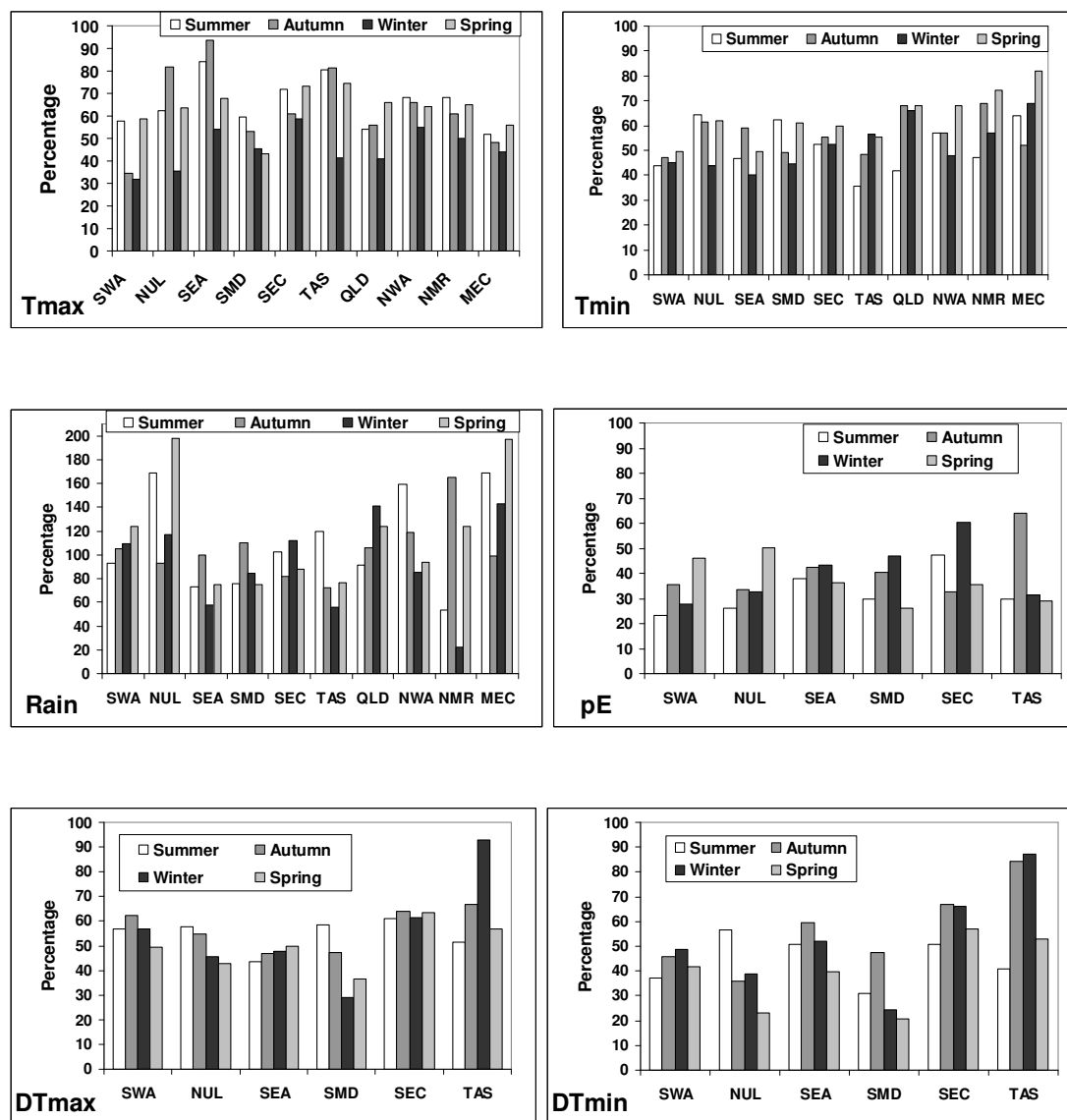


**Figure B5:** As per Figure B3 but for the percentage of the observed inter-annual variances reproduced by the reconstructed series.

Overall, the SDMs show a slightly better correlation on an inter-annual time-scale than on a daily timescale, but results are very consistent between the two time scales. The lowest correlation values are obtained for rainfall (albeit much improved compared to the daily time-scale) and highest for temperature. The seasonal variations of the results grossly resemble what was noted on the daily time-scale, but if anything they are slightly less obvious: either differences are smaller or consistency across regions is not as strong. For rainfall, the model is most able to reproduce inter-annual variability in winter (as was the case for daily variability) and in autumn for dew-point (that was also the case for daily variability). Although the correlations suggest

that the technique is able to capture most of the inter-annual variability, it appears to reproduce only a fraction of the inter-annual range (Fig. B5). Results are particularly low for pan evaporation (below 50% in most instances) and  $dT_{\min}$ . For  $T_{\max}$ , the percentage of reproduced variance is low in winter (30 to 60%) but mostly above 50% in other seasons. These seasonal differences are less pronounced for  $T_{\min}$ . For rainfall (note the different y-axis scale compared to the other variables), the percentage of observed variance reproduced is much higher, mostly between 60 and 100%, but exceeds 100% in several instances. Again, this is a flow-on effect of the correction factors applied to the reconstructed series, as earlier results showed that without the correction the reproduced inter-annual variability was underestimated for rainfall as well (Timbal, 2004).

Finally, an important validation step is to analyse the ability of the SDMs to capture observed long-term trends. This provides confirmation that the large-scale predictors capture the forcing that explains local trends and hence gives confidence in the ability of the SDM to reproduce realistic local changes driven by large-scale changes in future projections. Linear trends were fitted to all stations and regional averages are compared with similar trends from reconstructed series calculated for the length of the series: 1958 to 2003 for all predictands apart from pan evaporation (1975 to 2003) (Fig. B6). Each point on these graphs is a regional average of the available HQ stations, thus 24 points (four seasons and the six regions) are shown for  $dT_{\min}$ ,  $dT_{\max}$  and pE, and 40 points (four seasons and the ten regions) for  $T_{\max}$ ,  $T_{\min}$  and Rain. On each graph, the line of best fit (constrained to intercept with 0) between the observed and reconstructed series is shown (solid line) as well as the slope of the relationship and the correlation between the two variables (indicated in the bottom right corner of each graph). In general, the reconstructed series exhibit trends of a magnitude strongly related to the observed trends: the correlations vary between 0.87 for rainfall and 0.46 for  $dT_{\min}$ , suggesting that the SDMs have skill in reproducing the observed trends. However, the slope of these relationships is constantly less than one (between 0.14 and 0.57), pointing to an underestimation of the observed trend, which is of concern in regard to the ability of the SDM to reproduce the magnitude of the future changes.

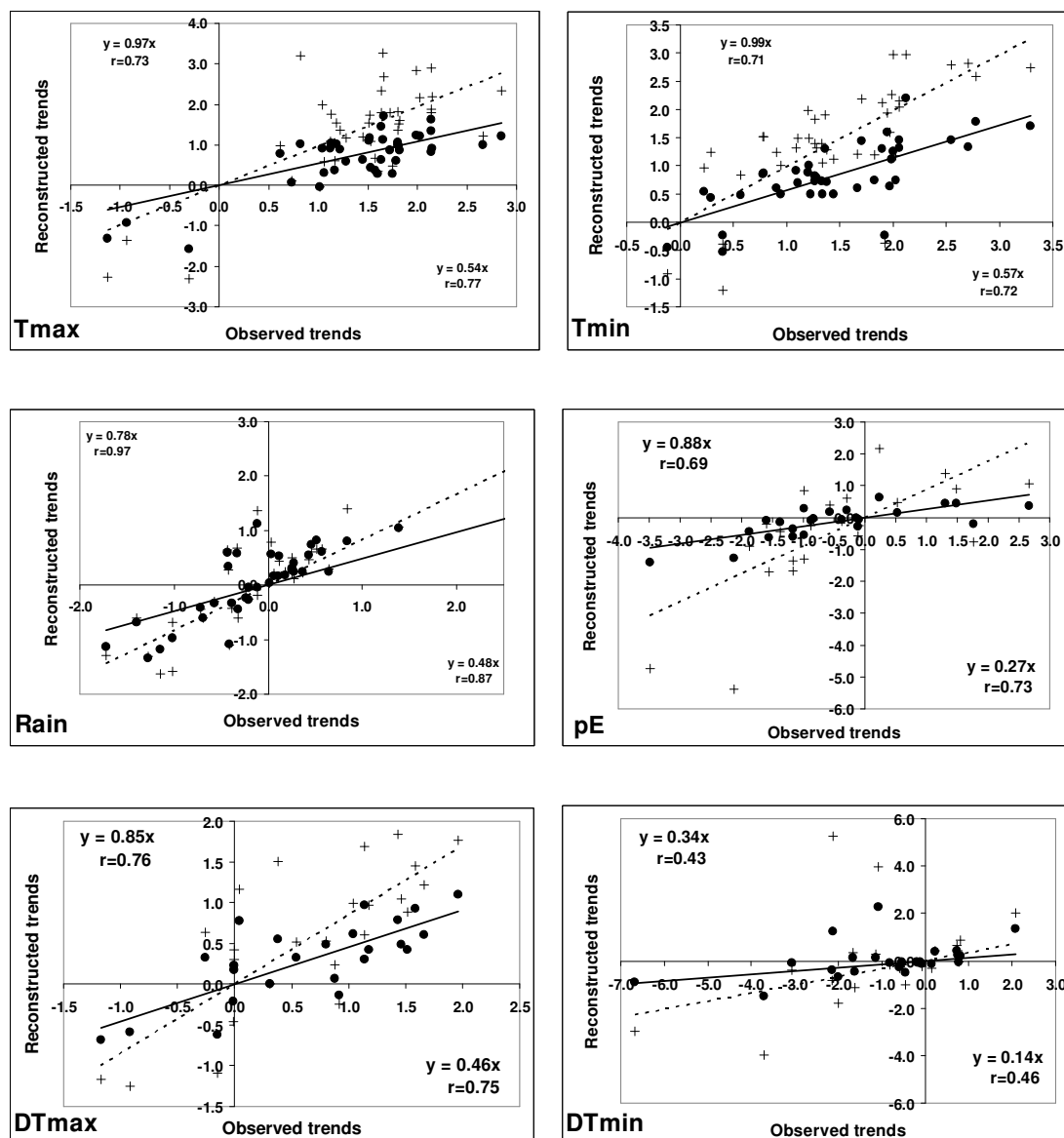


**Figure B6:** Scatter plot of the reconstructed versus observed linear trends fitted on the length of the longest possible record for the six predictands (dots) as well as for the normalised reconstructed trends (+ signs). For each series, there is one point per season and per regional average for all existing stations in that region. The total number of points per series is 24 for dTmin, dTmax and pE (six regions times four seasons) and 40 for Tmax, Tmin and Rain (ten regions times four seasons). The line of best fit is shown by the full (dashed) line and its slope as well as the correlation between the two variables in the bottom right (top left) corner for the original (normalised) reconstructed series.

However, since reconstructed series reproduced only part of the inter-annual range, it is expected that it would affect the linear trend fitted on the reconstructed series. The impact of this underestimation of the inter-annual variance can be shown by plotting the same graph for *normalised reconstructed series*, where the linear trend

is divided by the ratio of reproduced inter-annual variability (crosses in Fig. B6). Although the correlations between series (shown at the top left corners of the graphs in Fig. B6) remain by and large unchanged, the slope of the relationship in most cases is much closer to one, which is a major improvement with the notable exception of  $dT_{\min}$ . This latest finding enhances confidence in the model's ability to reproduce future climate changes at the local scale, as it is able to do so for the current climate changes. The result for  $dT_{\min}$ , however, casts doubt on the validity of future projections for this variable. All these findings should be considered by user when making use of projections data for impact studies.

*(Note: The trend plot for Rainfall (Fig. B6) has been cropped due to the presence of two outliers in region NMR in summer (slope = 13.60) and autumn (slope = 3.45). These outliers are taken into account when computing the correlations and slopes).*

## Appendix C: Perl scripts

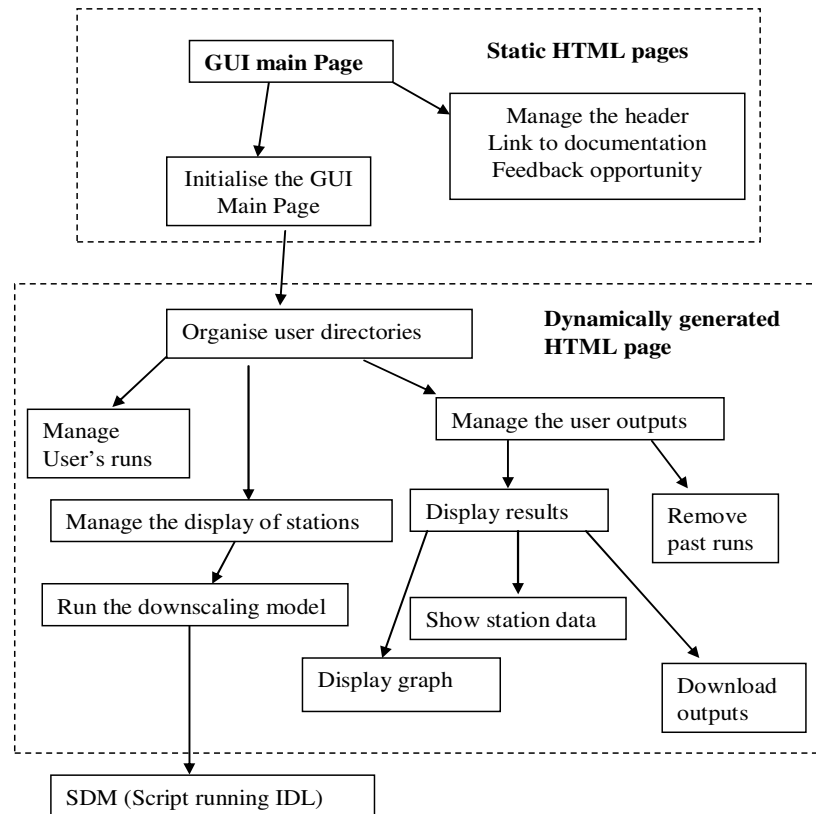


**Figure C1:** Flow chart of the GUI for the Bureau of Meteorology SDM.

### `x_startGUI.pl`

This is the starting point of the web interface. The first thing it does is to determine if there is any user directory available to store downscaling results. This program checks the cookie from the HTTP request to find out if this user is an old user. In that case, the user is given a previously assigned directory. Otherwise, a new cookie is set for

the user and a new directory is assigned provided there is still enough disk space available for an additional user. The cookie will expire after 24 hours.

The `getUserDir()` routine from the module `x_util.pm` is called from `x_startGUI.pl` to determine the user directory.

When the user directory is determined `x_makeGUI.pm` is executed to generate the web interface and `x_makeResultsTable.pm` is executed to generate the downscaling results table, empty at this stage.

### **x\_util.pm**

This is a utility module that contains routines that manage the user and the downscaling runs each user can make. It determines user directory and run directory. It is the program where the base directory can be modified.

### **x\_makeGUI.pm**

This module uses two languages to generate the GUI: HTML to build the text fields, drop-down menus and buttons, and JavaScript to generate the Google map (using Google map API) and allow the communication of Google map with the HTML forms. This module gets called whenever the GUI page is refreshed.

All available stations are hard-coded in this module to be displayed on the Google map. Google map API requires a signed-up key. The key is host-dependent and currently is for host 'gale.ho.bom.gov.au'. If the web interface is to be run on a different platform, a new key will have to be applied for and placed in this module. Details on how to get the key for Google map API can be found at <http://www.google.com/apis/maps/signup.html>.

**x\_run\_gstam.pl**

This program is executed once the button *Run Downscaling* is activated by the user. It specifies the run directory to be used, gathers all the options chosen by the user with the GUI and writes these in two files, `xoption.conf` and `xstn.conf`, stored in the run directory. `xoption.conf` contains all the options relevant to the choice of individual SDMs and hence the corresponding Change-Of-Date (COD) files for this particular run; `xstn.conf` contains the selected stations. These two files are accessed by the initial module of the SDM called by `xidldown_m` (in IDL language).

**x\_makeResultsTable.pm**

This module generates an HTML table to show the downscaling options, and creates a link to the downscaling results. It will open the `resultsTable.txt` file in the user directory to get the details of the user's chosen options displayed in the table, and to indicate where the downscaling results are located.

**x\_showResult.pl**

When the *Show Results* button in the downscaling results table is clicked, `x_showResults.pl` is executed. It generates a page in a new window that gives the downscaling results as a list of figures and data.

**x\_showFigure.pl**

When a figure in the list is highlighted, and the *Show Figure* button is clicked, `x_showFigure.pl` is executed, which will take the diagram in PS format and convert it into a GIF image to be displayed in the browser.

**x\_showData.pl**

When a data file in the list is highlighted and the *Show Data* button is clicked, `x_showData.pl` is executed, which will open the data file and display it in the browser.

**x\_download.pl**

When the *Download* link is clicked, all figures are converted to high-resolution PNG and zipped. The original PS file and data files also get zipped. A new page is generated to show the link of those zipped files, which can be downloaded.

**x\_deleteRun.pl**

If the *Delete this run* button in the downscaling results table is clicked, the results of this run will be deleted and the entry of this run in the `resultsTable.txt` of this user is set to `-1`, which means that this run directory is ready for storing results from another downscaling run.

**x\_deleteUser.pl**

Need to be (created/run?) to do the final clean up, exit the GUI and remove all stored data from the user after checking that it is OK (to be added to the flow chart)

## Appendix D: Directory structure

The base directory on Gale is `‘/bm/ghome/bxt/public_html/cgi-bin/gdownGUIresults’` and user directories are sub-directories. Due to the IDL licence limitation, up to three users are allowed to run the downscaling model at the same time. Therefore the user directory structure is as follows:

```
gale:/bm/ghome/bxt/public_html/cgi-bin/gdownGUIresults
-rwxrwxrwx  1 bxt      bmrc      129 Dec  5  18:24 user.txt
drwxrwxrwx  7 bxt      bmrc      1024 Nov 21  17:36 user1
drwxrwxrwx  7 bxt      bmrc      1024 Nov 21  17:36 user2
drwxrwxrwx  7 bxt      bmrc      1024 Nov 21  17:36 user3
```

`user.txt` contains limited information on the user, i.e. at what time the user started to use the GUI. This time is used to determine if this user, upon returning to the GUI after a while, should use an existing directory or get a new one. Currently, after 24hrs a user directory and all its contents are deleted to make space for other users.

Each user directory has five run sub-directories, allowing users to make 5 downscaling runs and store their outputs. Once 5 runs are performed, the user needs to delete old simulations in order to perform new ones (by clicking on the appropriate button for any of its five previous simulations):

```
gale:47 /bm/ ghome/bxt/public_html/cgi-bin/gdownGUIresults/user1
-rw-rw-rw-  1 zhl      bmrc      35 Mar 24  12:05 resultsTable.txt
drwxrwxrwx  2 zhl      bmrc      2048 Mar 24  12:05 run1
drwxrwxrwx  2 zhl      bmrc      2048 Mar 24  11:38 run2
drwxrwxrwx  2 zhl      bmrc      2048 Mar 20  14:35 run3
drwxrwxrwx  2 zhl      bmrc      2048 Mar 20  14:35 run4
drwxrwxrwx  2 zhl      bmrc      2048 Mar 20  14:35 run5
```

`resultsTable.txt` summarises information about the runs contained in each sub-directory:

```

1 1 NUL tmax 0 CCM_20C3M CSIRO_20C3M Forrest Woomera Tarcoola Marree Ceduna
1 2 -1
1 3 -1
1 4 -1
1 5 -1

```

The first column is the user number (1 in this example); the second column contains the run number; the third column shows all the options relevant to this run (region, scenario, stations ...) if the run has been completed otherwise it just displays -1.

All downscaling results (i.e. figures, text data and configuration files) are kept in individual run directories and their contents look like this:

```

gale:47 /bm/ ghome/bxt/public_html/cgi-bin/gdownGUIresults/user1/run1
-rw-r--r--  1 www      other      184164 Mar 24 23:19 ceduna_tmax_1.data
-rw-r--r--  1 www      other       1000 Mar 24 23:19 excel_inter_tmax_1
-rw-r--r--  1 www      other        150 Mar 24 23:19 excel_temp_mean1
-rw-r--r--  1 www      other        150 Mar 24 23:19 excel_trend_tmax_1
-rw-r--r--  1 www      other      184164 Mar 24 23:19 forrest_tmax_1.data
-rw-r--r--  1 www      other      85407 Mar 24 23:19 intervar_tmax_1.ps
-rw-r--r--  1 www      other      98167 Mar 24 23:19 m_pf_tmax1.ps
-rw-r--r--  1 www      other      70737 Mar 24 23:19 m_tmax_spell_cdr1.ps
-rw-r--r--  1 www      other      63885 Mar 24 23:19 m_tmax_spell_csd1.ps
-rw-r--r--  1 www      other      71556 Mar 24 23:19 m_tmax_spell_hdr1.ps
-rw-r--r--  1 www      other      57648 Mar 24 23:19 m_tmax_spell_hsd1.ps
-rw-r--r--  1 www      other      184164 Mar 24 23:19 marree_tmax_1.data
-rw-r--r--  1 www      other       10144 Mar 24 23:19 results_stm
-rw-r--r--  1 www      other      184164 Mar 24 23:19 tarcoola_tmax_1.data
-rw-r--r--  1 www      other      184164 Mar 24 23:19 woomera_tmax_1.data
-rw-r--r--  1 www      other        33 Mar 24 23:19 xoption.conf
-rw-r--r--  1 www      other        39 Mar 24 23:19 xstn.conf

```

xoption.conf and xstn.conf are two additional files generated by the GUI to store the options and chosen stations.

The base directory, user directories and run directories currently are granted read, write and execute privilege for user, group and others as GUI users are *www*

(web server) and belong to the *others* group. This level of permissions for *other* is needed in order to save the files.

## Appendix E: The Statistical Downscaling Model (SDM)

The SDM has been designed to be completed in two parts: a computing intensive part which deals with the treatments of the predictors up to the selection of the analogues stored in the Change-Of-Date (COD) files, and a second part to perform calculations for the reconstructed predictands and generate plots comparing reconstructed and observed series (Fig. E1). The details on each subroutine performing the function described above are given in Figure E2 and the subsequent text.

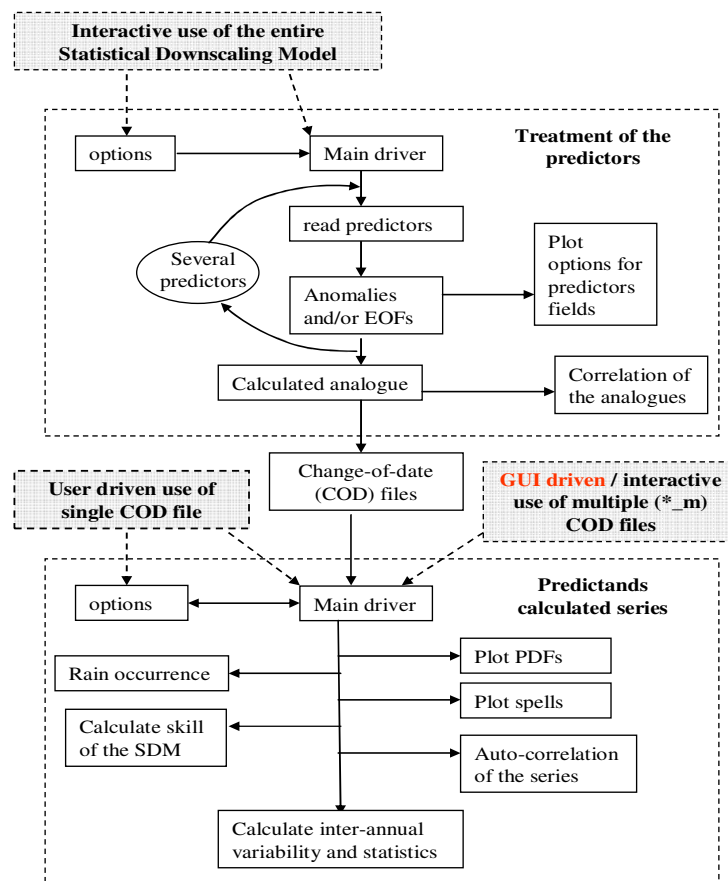


**Figure E1:** Flow chart of the structure of the Bureau of Meteorology SDM.

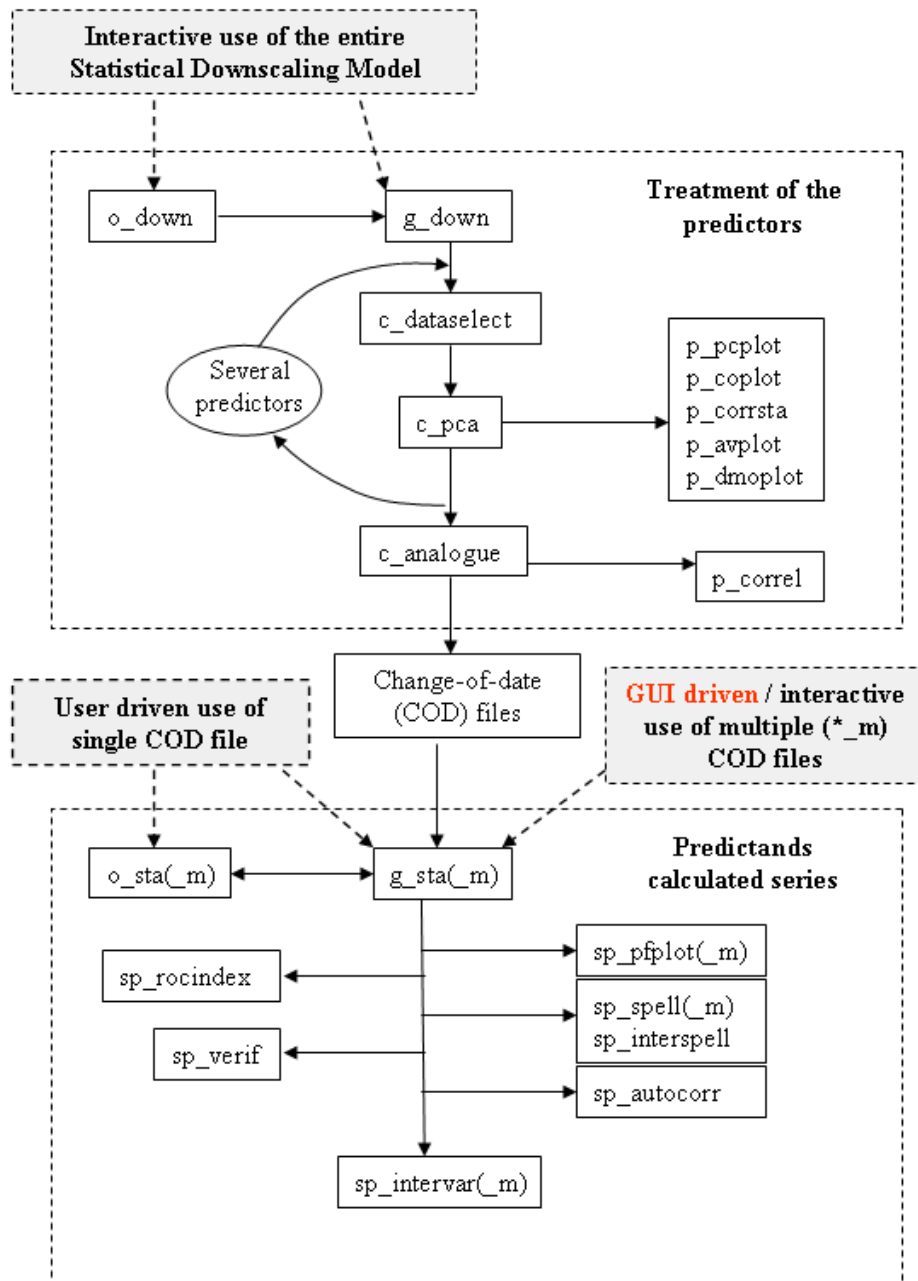


**Figure E2:** Flow chart of the subroutines within the Bureau of Meteorology SDM. The file names starting with *o\_* denote options files, *g\_* denotes general subroutines, *c\_* denotes calculation on the predictor's fields, *p\_* denotes subroutines to plot predictor results and *sp\_* denotes calculations on surface predictands. Files with *\_m* suffix denote subroutines where multiple use of change-of-date files is possible.

Scripts to run the SDM are called *xidl\**: *xidldown* is used to run the entire model from the treatment of the predictors to the calculation of the analogues (COD files) and the treatment of the predictands. Options exist to use this script and re-run

predictands calculations while using an existing COD file. `xidlsta_m` is used when COD files already exist and several are to be used (to compare outputs from different SDM projections or the downscaling of several climate models).

### **o\_down.pro**

This subroutine contains all the options to run the SDM relevant to the choice of predictors and parameters of the models. The code contains several notes detailing the choices regarding:

1. the choice of model simulations;
2. the available predictors;
3. the existing choice of predictands;
4. the different regions of interest; and
5. the options for choosing a season.

### **g\_down.pro**

This is the main part of the SDM; it receives from `o_down.pro` the user-defined options to run the statistical model and calls the subsequent procedures to analyse the predictor's fields (looping over the number of predictors chosen) before calling the subroutine to calculate the analogue and finally calling the procedure to treat the predictands.

### **c\_dataselect.pro**

This subroutine reads the binary files containing any model (reanalyses, IPCC models, other) fields and extracts the appropriate window as defined by the user in `o_down.pro`. If necessary the model grids are interpolated to be comparable with the reanalyses.

### **c\_pca.pro**

This subroutine calculates normalised anomalies from the model fields according to some options chosen by the user:

1. the base climatology: validation/control/scenario;
2. what type of anomalies: monthly/ seasonal/spatial; and
3. whether to detrend the data or not.

Then the procedure will plot, if required, the mean and standard deviation of the predictors. Finally, if required, the code will calculate the leading Empirical Orthogonal Functions (EOFs) onto which the analogues are to be calculated unless the option `rawfield` has been selected for the choice of analogue.

### **p\_\*.pro**

These subroutines generate some plots of model predictors:

- ✓ `p_avplot.pro`: mean and variance of any predictor field;
- ✓ `p_pcplot.pro`: the leading PCs;
- ✓ `p_coplot.pro`: the loading of the leading PCs;
- ✓ `p_corrsta.pro`: spatial correlation of a field with a local observation; and
- ✓ `p_dmoplot.pro`: model predictors plotted using grid boxes instead of smooth lines

### **c\_analog.pro**

This is the subroutine where the analogues are calculated once the predictors have been prepared according to the chosen options. The calculation of predictors can be achieved using different methods. Results are achieved in the COD files and several analogues can be archived.

### **p\_correl.pro**

Once analogues have been calculated, this procedure can plot the spatial correlation between a day and its analogue averaged across all dates considered.

### **o\_sta.pro**

This subroutine contains all the options relevant to the predictands. It can be accessed as a standalone, once the calculation of the analogue is completed, to run the SDM relevant to the choice of predictors and parameters of the models. `o_sta_m.pro` is the same subroutine but set up to run through several COD files when used interactively. This subroutine is accessed by the GUI and supplied with the user options.

### **g\_sta.pro**

This is the main code for the treatment of the predictands. Reconstructed series based on the choice of analogue (stored in the COD files) are generated here. Then the code calls a series of subroutines to calculate statistics and generates plots for local predictands. The version that deals with multiple COD files is `g_sta_m.pro`.

### **sp\_pfplot.pro**

This procedure plots PDFs of the reconstructed and observed series for near Gaussian series (temperature, dew point, evaporation). There is a separate subroutine (`sp_pfplotprec.pro`) to plot accumulated PDFs for rainfall. Both subroutines have an `_m` option to plot multiple results.

### **sp\_spell.pro**

This procedure plots spell durations and inter arrival times (between events). An `_m` option exists to plot multiple results. In addition there is a procedure to plot inter-annual variability of the number of fixed spells: `sp_interspell.pro`.

### **sp\_rocindex.pro**

This procedure calculates statistics on the reproduction of rainfall occurrences (WMO index, hit rate ...). It is mostly useful during the validation phase of the SDM.

### **sp\_verif.pro**

This procedure calculates a range of statistics on the ability of the SDM to reproduce observed series (correlation, root mean square error, biases). It is mostly useful during the validation phase of the SDM.

**sp\_autocorr.pro**

This procedure calculates the auto-correlation of the reconstructed series and compares it to the observed series. It also calculates the probability of an event following the same event (such as rain occurrences).

**sp\_intervar.pro**

This procedure plots inter-annual variability of the reconstructed series compared to the observed one (calculations for that plot are done within the `g_sta.pro` subroutine). There is an `_m.pro` version to plot multiple results.

Additional subroutines and utilities exist to help manage some of the outputs of the SDM code.

## Appendix F: The graphical outputs

Upon completion of the downscaling calculation, the user can access several graphical outputs, depending on the predictand downscaled. In all cases, an inter-annual variability plot is generated, as well as a probability density function (PDF) plot for temperature variables or a cumulative distribution function (CDF) plot for rainfall. In addition, some figures are available to describe the probability of extreme duration of particular spells.

On each of these plots, the thick black curve represents the observations and the red curve(s) the downscaled series (one per model). When results are plotted for the 20<sup>th</sup> century (1960-1999), the observations are the true observations for that 40-years period. However, for future projections (20 years period either in the middle or at the end of the 21<sup>st</sup> century), the black curve is constructed using past observations for a reference 20-years period: 1975 to 1994.

Some statistics are provided in each graph for both the observations and the range of future projections. The range is expressed across the selected GCMs (i.e. highest and lowest value are identical if only one GCM is used (see figure F3 for an illustration), and will encompass a broader range of uncertainties as more GCMs are used. When several statistics are shown on a plot, highest and lowest values are independent from one another: i.e. the highest values are not necessarily from the same GCM.

In the case of temperature, a PDF is plotted (Fig. F1). It represents the distribution of the observations and the downscaled results. Some statistics are available on the figure; for the observations, these are the mean (Mean), variance (Var), minimum (Mn) and maximum (Mx) values. Below the same statistics are repeated for the downscaled results: M+ (M-) is the highest (lowest) mean among the models used, V+ (V-) is the highest (lowest) variance, Mn+ (Mn-) is the highest (lowest) minimum, and Mx+ (Mx-) is the highest (lowest) maximum.

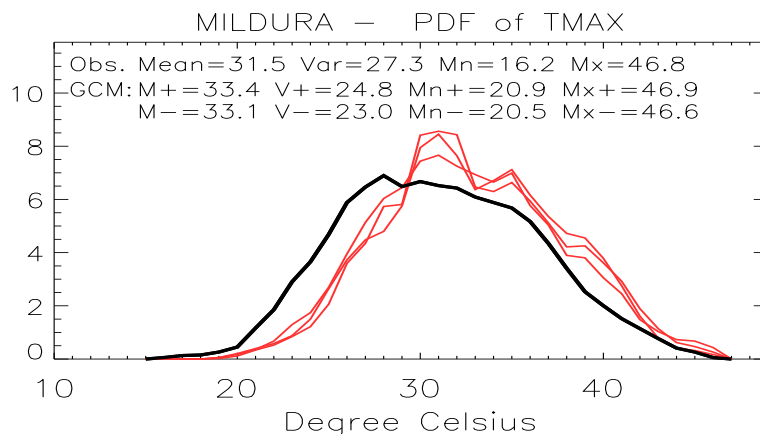


**Figure F1:** Probability density functions of maximum temperature in summer in Mildura (region SMD) for the middle of the 21<sup>st</sup> century (2046 to 2065), using emission scenario A2 for CSIRO, CCM and CNRM models.

For rainfall, a CDF rather than a PDF is plotted (Fig. F2). Some statistics are provided in the graph, for the observations (first line) and for the range of future projections: the percentage of dry days (%D), the average rainfall intensity (AI) and the median rainfall (R50) for rainy days, and the total rainfall (TR). A rainy day is currently defined as a day with at least 0.3mm of precipitation, but this threshold can be modified in the code.

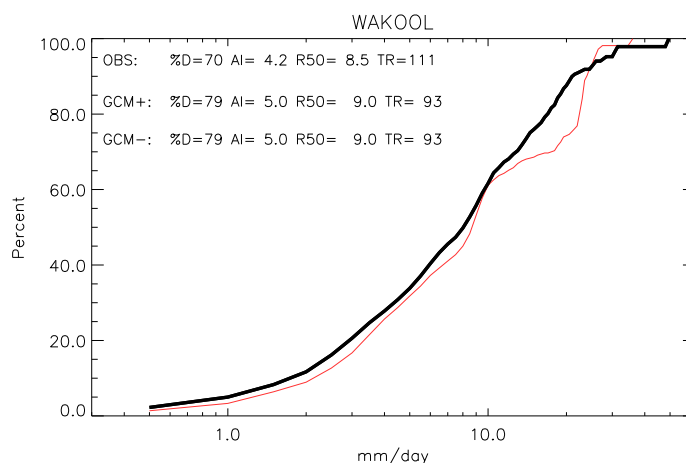


**Figure F2:** Cumulative distribution functions for rainfall in winter in Wakool (region SMD) for the end of the 20<sup>th</sup> century (2081 to 2100), using emission scenario A2 for the CSIRO model. The x-axis (logarithmic scale) represents rainfall in mm/day and the y-axis the corresponding probability in percent.

An inter-annual variability plot (Fig. F3) is also generated whenever surface predictands are chosen. It depicts the year-to-year evolution of the seasonal mean temperatures or seasonal total rainfall across the period considered, as shown in Figure F1 for summer Tmax in Mildura from 2046 to 2065. Some statistics are available on the figure; for the observations, the mean for temperature or total for rainfall (Mean), range (Range) (i.e. the difference between the highest and lowest seasonal means) and slope (Slo.) (i.e. the slope of the linear regression fitted to the observations). Then the same statistics are provided for the downscaled results: M+ (M-) is the highest (lowest) mean among the models used, R+ (R-) is the highest (lowest) range, and Sl+ (Sl-) is the highest (lowest) slope.

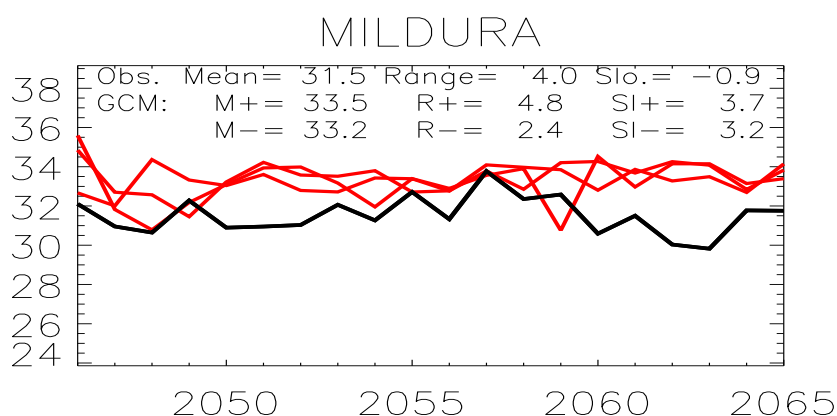


**Figure F3:** *Inter-annual variability of maximum temperature in summer in Mildura (region SMD) for the middle of the 21<sup>st</sup> century (2046 to 2065), using emission scenario A2 for CSIRO, CCM and CNRM models. The x-axis represents the years of observations/projections, the y-axis the average temperature in degrees Celsius.*

Finally, in order to document the ability of the technique to reproduce extreme events, the probability of duration of anomalous long-spells are shown:

- Dry and wet spell for rainfall;
- Hot and cold spells for temperature as well as return period for hot and cold days.

For rainfall, a wet spell duration (WSD) is defined as the number of consecutive days with rainfall recorded in excess of 0.3mm. This threshold can be modified within the

code and could become an option chosen by the user. Similarly, dry spell durations (DSD) are being plotted using the same threshold (0.3mm) to define dry days.

For temperature, hot and cold spell durations (HSD and CSD) are plotted (see an example for HSD, left diagram in Fig 4) as well as hot and cold day return periods (HDR and CDR, see an example for HDR, right diagram in Fig 4). A hot spell of  $n$  days is defined as a series of  $n$  consecutive days with temperature exceeding a threshold; a cold spell is similarly defined as a series of  $n$  days with temperatures below a defined threshold. The threshold is defined separately for each series (observations or downscaled models); it is currently defined as the mean plus the variance for a hot spell, the mean minus the variance for a cold spell. This threshold can be modified in the code depending on user needs. The values for the thresholds are shown on the plots for the observed series as well as the lowest (GCM-) and highest (GCM+) thresholds used for the models. Return period plots represent the probability of the duration, in number of days, between two events: two hot days for hot day return or two cold days for cold day return. Similar thresholds to those for duration are used for return period.

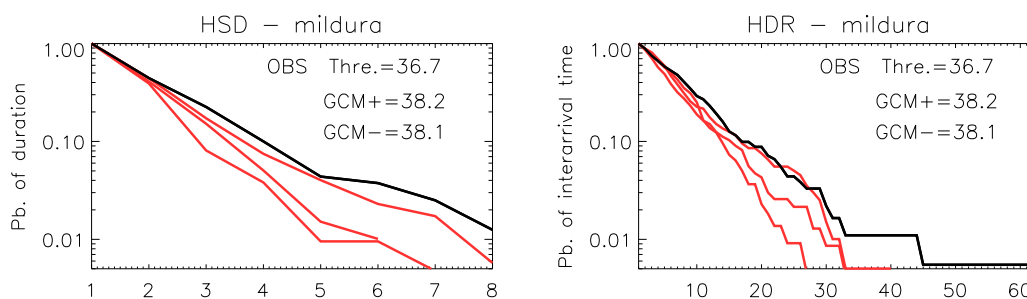


**Figure F4:** Probability of hot spell duration (left) and hot day return (right) for maximum temperature in Mildura (region SMD) for the middle of the 21<sup>st</sup> century (2046 to 2065), using emission scenario A2 for the CSIRO, CCM and CNRM models. The x-axis represents the number of days, the y-axis (logarithmic scale) represents the probability of duration on the left plot, and the return period on the right plot.

## Appendix G: Case study 1: projected Tmax in Mildura

To illustrate the usefulness of the BOM-SDM as a tool to obtain detailed point-specific climate change projections, a case study was completed using the GUI. In this example, maximum daily temperatures in summer were sought for Mildura in the northwest of Victoria (within the SMD region), which is an important regional centre in particular for agriculture. Additional case studies for both temperature and rainfall can be found in the Climate Change in Australia report (BoM and CSIRO, 2007).

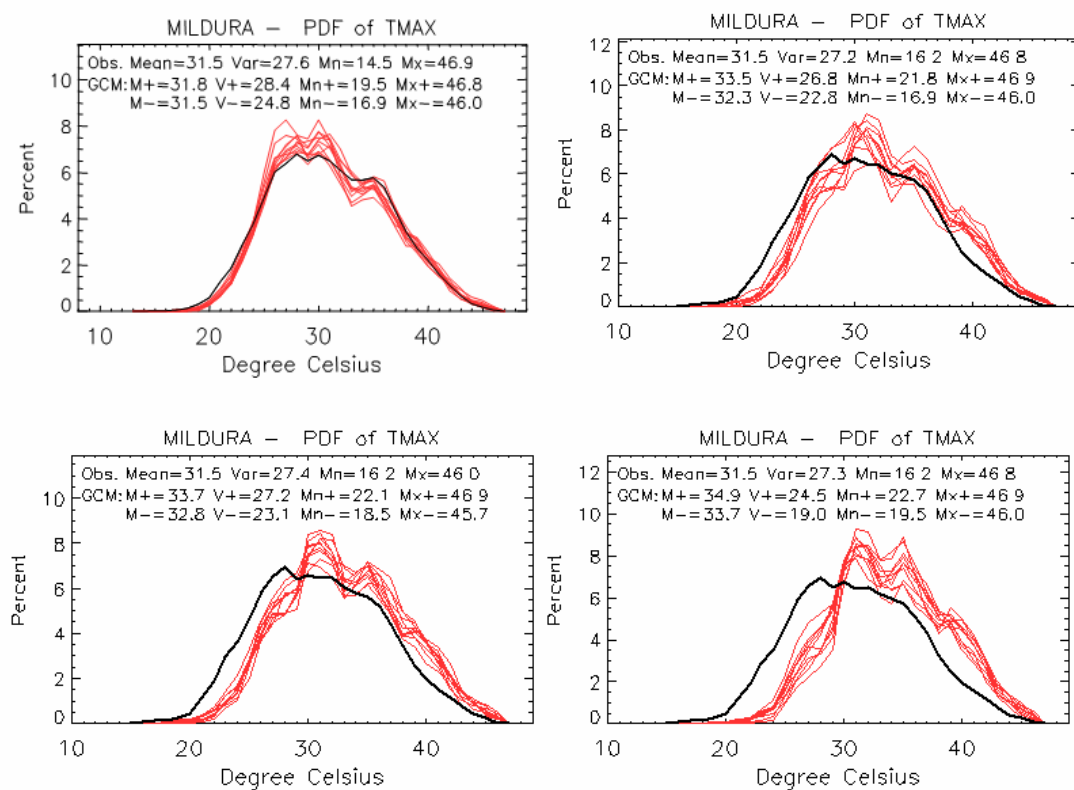


**Figure G1:** Probability density functions of maximum temperature in summer in Mildura (Victoria, located in SMD) for the end of the 20<sup>th</sup> century (top left) and for the middle of the 21<sup>st</sup> century using emissions scenario B1 (top right). Similar plots show the scenario A2 for the middle (bottom left) and the end of the 21<sup>st</sup> century (bottom right). Observations are shown as a thick black line, and the downscaling of each of the 10 individual climate models from the CMIP3 database are shown as red lines. Mean, variance, and maximum and minimum of the series are shown on the graphs as the top text line, followed by the range of the same statistics across the 10 downscaled models.

The downscaling of all climate models provides a good estimate of the local PDF for  $T_{\max}$  in summer in Mildura (Fig. G1, top left). The mean and variance from the downscaling of the GCMs encompass the observed values (observations statistics are shown on the top line in each diagram, while the model range is given in the following two lines). It is worth noting that the particular shape of the PDF, with a broad maximum around 28°C and a secondary maximum around 35°C, is also captured. The transformation of the PDF under future projections is shown for 2050 for the B1 (Fig. G1, top right) and A2 scenarios (Fig. G1, bottom left), and for 2100 for the A2 scenario (Fig. G1, bottom right), in this order the graphs look at the details warming as a function of the magnitude of the forcings and the global warming. It is worth noting that the observed PDFs are not strictly identical (nor are the statistics for the observations) in the case of the 20<sup>th</sup> century and for future projections. This is due to the different baselines: 1960 to 1999 for the 20<sup>th</sup> century and 1970 to 1989 for future projections.

One of the criticisms often made about downscaled climate change projections is that it is not possible to validate the underlying assumption that the statistical linkage remains valid in a warmer world (Hewitson and Crane, 2006). This point was partially answered during the model evaluation stage by showing that the SDMs were able to reproduce the observed trends. In this case study, it is possible to compare the point-specific projections with direct model projections coming from the CMIP3 models for grid boxes surrounding Mildura (documented in the Climate Change in Australia report, BoM and CSIRO, 2007 and available online at <http://www.climatechangeinaustralia.gov.au/>). Although this comparison is not a perfect match because numbers are coming from very different methodologies, it provides an interesting overview of the consistency among these different projections.

For 2050, direct model projections suggest a range for high emissions scenarios between 1 and 1.5°C at the 10<sup>th</sup> percentile, 2 and 2.1°C at the 50<sup>th</sup> percentile and 2.5 to 3°C at the 90<sup>th</sup> percentile, and for low emissions scenarios, between 0.6 and 1°C at the 10<sup>th</sup> percentile, 1 to 1.5°C at the 50<sup>th</sup> percentile and 2 to 2.5°C at the 90<sup>th</sup> percentile. These values are comparable with the suggested warming of 1.3 to 2.2°C shown here for the A2 scenario (a high emissions scenario) and 0.8 to 2°C for the B1 scenario (a

low emissions scenario). The range is not as large as with the direct model outputs but in that case the entire CMIP3 database (23 models) were used compared with only 10 models in our case study, and the low and high emissions scenarios in the CSIRO and BoM (2007) projections are based on more than the single scenario (B1 or A2) used here.

In addition to the mean local warming and the changes of the PDF, it is possible to take a closer look at the details that the local warming implies. For example, the length and duration of hot spells (number of consecutive days above a particular threshold) can be looked at. The downscaling of the climate models underestimates the hot spell duration (Fig. G2).

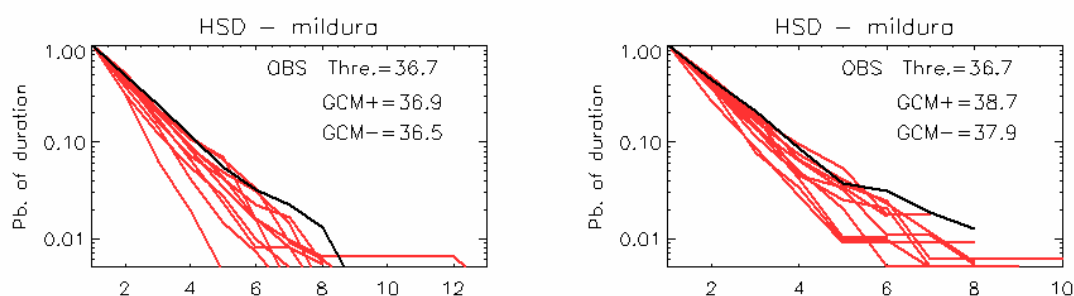


**Figure G2:** Hot spell duration expressed as the probability of having a certain number of days exceeding a certain threshold for  $T_{max}$  in summer in Mildura for the end of the 20<sup>th</sup> century (left) and for the middle of the 21<sup>st</sup> century using emissions scenario A2 (right). Observations from 1960 to 1999 are shown as a thick black line on the 20<sup>th</sup> century diagram; for the 21<sup>st</sup> century case the period 1970 to 1989 is used to provide a reference for the downscaled model simulation for 2046 to 2065. The thresholds used depend on the mean and variance of the series, and differ from observations to models and from the 20<sup>th</sup> century to the 21<sup>st</sup> century as shown on the graphs.

For example, the observed probability that hot spells above 36.7°C last up to 8 days is about 0.01 in Mildura. The same probability for the downscaled model suggests a spell length between 5 and 7 days (left graph in Fig. G2), but the threshold used (which depends on the mean and variance of the individual series) matches the observed threshold. Keeping these results in mind, future projections of hot spell duration show that much larger thresholds are used (due to the mean warming) but the

probability of spell length is hardly changed. Also, there is an indication that longer spells could become more likely, as model curves are slightly more clustered toward the observed trend than they were in the current climate case; but this may not be significant as it is likely to be by less than a day apart for more extreme spells (right graph in Fig. G2). Of course, if the threshold used for the 20<sup>th</sup> century were kept, results would be very different as days above 36.7°C are projected to be far more frequent (as implied by the PDFs in Fig. G1). Looking at hot spell duration using a threshold fitted to the new distribution implies that the population and the environment would have adapted to the mean warming. However, as users can access ASCII files with the daily values used to construct the PDFs, they can perform additional analyses on extremes and decide on which thresholds to use. The graphs generated by the GUI (Figs. G1 and G2) serve to illustrate the main characteristics of the downscaled results and the possibility of generating many analyses, as the locally constructed daily series (in the 20<sup>th</sup> century climate) are highly realistic.

When dealing with extremes and using downscaled projections, it is important to keep in mind that the statistical linkage established using the data is more likely to be robust for the middle of the distribution, for which there are more observations, than for the extremes which are not so extensively sampled. For example, since the SDM uses an analogue approach, it is not possible to get daily projected values that have not been observed before (e.g. new record temperatures). In the case study, the maximum value is tied to the past record in summer observed at Mildura during the 1958 to 2003 period: 46.9°C. That explains why despite the mean warming (e.g. for A2\_100, bottom right in Fig. G1), the upper tail of the distribution does not shift right with the rest of the distribution. This situation can be contrasted with what is happening for record low temperatures, shifting from 16.2°C to between 19.5 and 22.7°C, a massive increase of up to 6.5°C by 2100 with the A2 scenario (compared to the lowest value observed between 1970 and 1989). Similar shifts might be a reasonable assumption for record hot temperatures, but it is not possible to infer this from the current set of results. Therefore, in the case of warm extremes, only the frequency of occurrences below the local record temperature would be meaningful for future projections.

## Appendix H: Case study 2: sub-grid heterogeneity

### a) For temperature

Climate models provide grid-box averages (Skelly and Henderson-Sellers 1996). Due to the coarse resolution of most climate models, uniform information is given for a large area and therefore sub-grid heterogeneity is not captured. Hence future projections do not provide these local details which are highly important to understanding the impact of projected climate change on the natural and man-made environment.

The importance of local differences across a geographical region represented by a grid box of a global climate model is illustrated in Figure H1. It shows probability density functions of temperature change for four locations in southeast New South Wales that could easily fit within a single grid box. This area encompasses part of the Great Dividing Range.

The results show notable differences from one part of the grid box to another: in Jervis Bay near the coast it is expected to be between 0.5 and 1.0°C, while in Canberra the expected warming is more than twice as large (between 1.1 and 2.3°C). The warming is slightly larger further inland (Wagga-Wagga), and even larger for higher elevation (Cabramurra). The increased warming away from the coast is a well known and expected feature depicted by GCMs; the additional warming with elevation is less documented as it is usually not captured by GCMs which have a limited ability to reproduce the orography due to coarse model resolution.

The projected warming is broadly similar with direct model outputs for the area (between 1.4 and 1.8°C). Although direct model outputs provide a hint that coastal warming is expected to be lower than further inland, the downscaled results provide a more contrasting response.

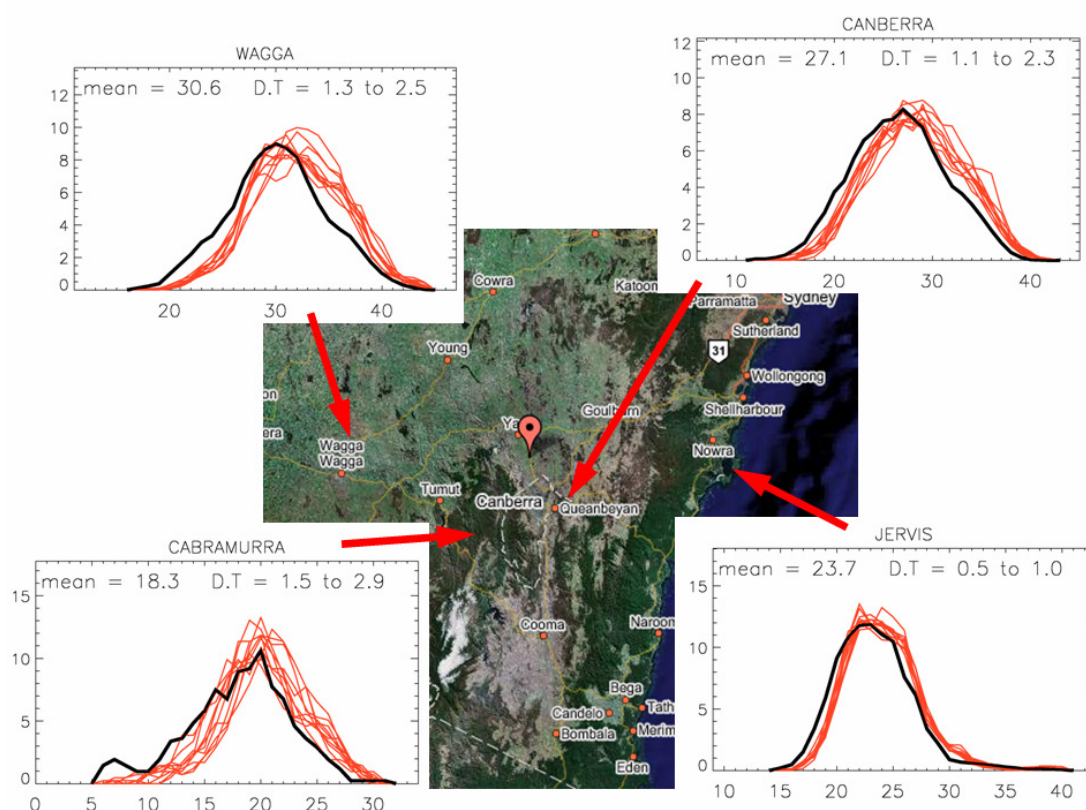


**Figure H1:** Projected changes of the observed probability density functions of maximum temperature in summer for 2050 (using emissions scenario A2) in four neighbouring locations with contrasting climates: Jervis Bay (a coastal location), Canberra (150 km inland, in the Great Dividing Range but at low elevation), Cabramurra (inland, at high elevation) and Wagga-Wagga (on the western side of the Great Dividing Range) using the statistical downscaling technique described in the text. Observations are shown as thick black lines, the 10 individual climate models from the IPCC AR4 database are shown as red lines.

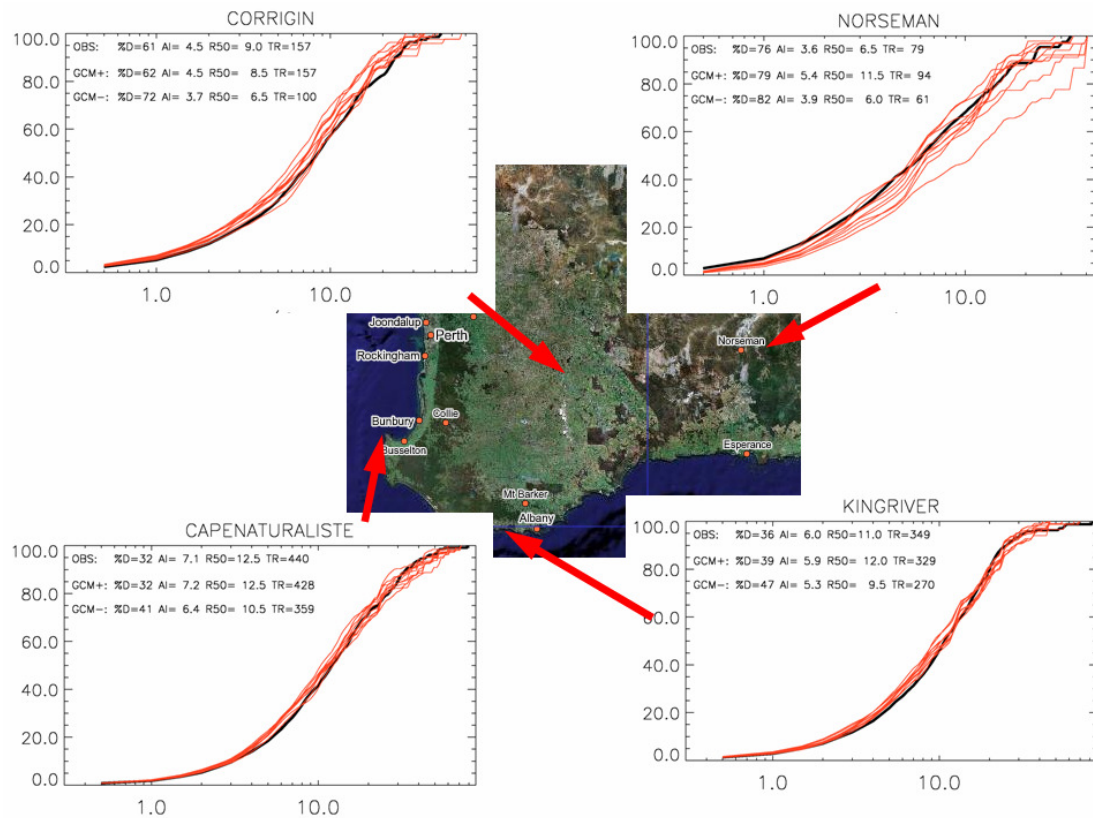
It is also possible to estimate the chances that the warming will exceed fixed thresholds such as 1.5°C. This probability varies markedly across the grid box as expected from the warming range projected at each location: it is less than 5% in Jervis Bay but reaches 80% in Canberra and Wagga-Wagga; and it exceeds 95% in Cabramurra.

**b) For rainfall**

Sub-grid scale heterogeneity can also be particularly important for rainfall, which is spatially highly variable. This result was illustrated for the southwest of Western Australia which has suffered one of the most severe rainfall declines in recent history (Ryan and Hope 2005, 2006).

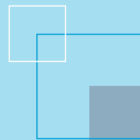
Future projections based on the A2 scenario for winter (June to August) rainfall (Fig. H2) indicate a further rainfall reduction of the total rainfall (TR on the graphs), alongside a reduction of the average rainfall intensity (AI), a reduction of the rainfall intensity for the middle of the distribution (R50), and an increase of the percentage of dry days (%D). There is a high level of consistency among models. They all suggest a decline in total rainfall in this part of Western Australia from the coast (between 3 and 22% in Cape Naturaliste and King River) to the inland wheat belt (between 0% and 36% in Corrigin). On the contrary, further inland (Norseman), the rainfall is more likely to increase (as projected by 6 models) than to decrease (projected by only 4 models). This difference between the southwest corner and further inland is consistent with the direct model outputs projections (Bom and CSIRO, 2007), but with a sharper contrast.

As was the case for temperature, the statistical downscaling product has the ability to show notable differences within small distances, consistent with the broad picture provided by GCM direct outputs but with a sharper contrast. In addition, as the full distribution at each location provided is given, a range of statistics such as those discussed earlier can be obtained to help characterise the nature of the mean rainfall changes.



**Figure H2:** Projected changes of the observed cumulative probability distributions of Australian rainfall in winter for 2050 (using emissions scenario A2) in four locations in the southwest of Western Australia, with contrasting climate: Cape Naturalist (along the west coast), King River (along the south coast), Corrigin (in the heart of the wheat belt) and Norseman (further inland). Observations, based on the 1970 to 1989 period, are shown as thick black lines. Ten individual climate models from the IPCC-AR4 database are shown as red lines. The x-axis in mm used a logarithmic scale while the y-axis is expressed in percent. Some statistics extracted from the cumulative distribution are provided for the current climate (first line in each insert) and for the range of future projections (largest rainfall on the second line and smaller rainfall on the third line). The meaning of each statistics is discussed in the text.





The Centre for Australian Weather and Climate Research is a partnership between CSIRO and the Bureau of Meteorology.